

A STUDY OF THE DIAGENESIS OF THE LOWER CRETACEOUS,
NITON BASAL QUARTZ SANDSTONES OF WESTERN ALBERTA;
WITH SPECIFIC REFERENCE TO POROSITY AND
PERMEABILITY MODIFICATION

A STUDY OF THE DIAGENESIS OF THE LOWER CRETACEOUS,
NITON BASAL QUARTZ SANDSTONES OF WESTERN ALBERTA;
WITH SPECIFIC REFERENCE TO POROSITY AND
PERMEABILITY MODIFICATION

BY

DANIEL JOHN POTOCKI

A THESIS SUBMITTED TO THE DEPARTMENT OF GEOLOGY
IN PARTIAL FULFILLMENT OF THE REQUIREMENTS FOR THE
DEGREE HONOURS BACHELOR OF SCIENCE.

McMASTER UNIVERSITY

1981

Honours Bachelor of Science
(Geology)

McMaster University
Hamilton, Ontario

TITLE: A Study of the Diagenesis of the Lower Cretaceous,
Niton Basal Quartz Sandstones of Western Alberta;
With Specific Reference to Porosity and
Permeability Modification

AUTHOR: Daniel John Potocki

SUPERVISOR: Dr. G. V. Middleton

NUMBER OF PAGES: xi, 83

ABSTRACT

Abnormal accumulations of kaolinite and illite clay minerals, significantly reducing reservoir potential in localized portions of the Niton Basal Quartz sandstones, have prompted a detailed examination of the (clay) mineralogy and diagenetic history of these sands. Scanning electron microscopy and thin section analysis show that the bulk of porosity reduction is by the accumulation of detrital clays in sands where insufficient winnowing has occurred during deposition in the deltaic environment. The progressive assemblage of authigenic quartz overgrowths, authigenic illite and authigenic kaolinite further reduce porosity and permeability during diagenesis. Secondary kaolinite tends to infill sands of high initial porosity. Oil migration occurs after the formation of authigenic kaolinite and minor amounts of dissolution porosity. Clay accumulations reduce but do not destroy reservoir potential of the Niton Basal Quartz sandstones.

ACKNOWLEDGEMENTS

The author would like to express his gratitude to Dr. G.V. Middleton who supervised the production of this thesis, and introduced the author to the fine art of 'ruthlessly excluding waffle'.

Esso Resources Ltd. is also acknowledged for supporting the author in the early stages of the thesis. The following personnel from Esso deserve special recognition. Peter Byers for his efforts in helping to find an interesting thesis topic. Discussions with Hans Nelson and Perry Glaister in developing the thesis topic were very much appreciated, and special thanks go to Dave James for time devoted in making the summer at Esso a true learning experience.

Also acknowledged for their able assistance are Jack Whorwood for photographic assistance, and Len Zwicker for preparation of thin sections. Janet Lawson deserves special recognition for patiently typing the manuscript.

To
my Mother, Father,
Helen and Mary

TABLE OF CONTENTS

	<u>Page</u>
Abstract	
Chapter 1	
Area of Study and Statement of Problem	1
General Stratigraphy	4
Depositional Framework, Regional and Local	5
Regional	5
Local Depositional Framework	8
Chapter 2	
Local Stratigraphy and Facies Description	11
Introduction	11
Facies Descriptions	13
Introduction	13
Laminated Mudstone/Siltstone Facies (L.M.S.)	13
Bioturbated Mudstone/Siltstone Facies (B.M.S.)	19
Sandstone Facies (S.S.)	19
Bioturbated Sandstone Facies (B.S.S.)	20
Silty Sandstone Facies (S.L.S.S.)	22
Coquinoid Sandstone Facies (C.S.S.)	22
Interpretations	23
Chapter 3	
Petrographic Observations	27
Thin Section Observations	27
Introduction	27
Composition	27
Quartz Grains	29
Calcite	32
Feldspar	32
Glauconite	32
Other Minerals	34

Chapter 3	Continued	Page
	Clay Mineralogy	35
	Introduction	35
	X-ray Diffraction	35
	Identification of Clay Minerals	35
	Sample Preparation	36
	Kaolinite	37
	Illite	37
	Petrographic Thin Section and Scanning	
	Electron Microscope	40
	Differentiation of Clay Minerals	40
	Sample Preparation	40
	Detrital Illite	41
	Detrital Kaolinite	41
	Authigenic Illite	43
	Authigenic Kaolinite	47
	Semiquantitative Analysis	52
	X-ray Diffraction Results	52
	Thin Section Visual Estimates	55
Chapter 4	Petrographic Interpretations	56
	Mineralogic Maturity	56
	Textural Maturity	56
	Provenance	57
	Detrital Illite	58
	Detrital Kaolinite	59
	Porosity Reduction By Clay Minerals	60
	Detrital Clays	60
	Authigenic Clays	61
	Prelude to Paragenesis	62
	Determination of Geothermal Gradient	63
	Determination of Maximum Burial Depth	63
Chapter 5	Diagenesis	67
	Introduction	67
	Eodiagenesis	67
	Mechanical Reduction of Porosity	67
	Pore Fluid Chemistry	68
	Pyrite Formation	69
	Siderite Formation	70
	Mesodiagenesis	70
	Authigenic Quartz Overgrowths	70
	Authigenic Illite	71
	Authigenic Kaolinite	75
Chapter 6	Conclusions	82
Appendix I		
Bibliography		

LIST OF FIGURES

	Page	
Figure 1.1	Location Map	2
Figure 1.2	Stratigraphic Nomenclature	6
Figure 1.3	Isopach of Lower Cretaceous Strata in Central Alberta	7
Figure 1.4	Niton Basal Quartz "B" Pool Isopach Map	9
Figure 2.1	Stratigraphic Section and Porosity Permeability Data 10-14-54-13W5	15
Figure 2.2	Stratigraphic Section and Porosity Permeability Data 4-30-54-12W5	16
Figure 2.3	Stratigraphic Section and Porosity Permeability Data 2-18-54-12W5	17
Figure 3.1	Sandstone Classification Diagram	30
Figure 3.2	X-ray Diffraction Peaks Sample 4-30-4	38
Figure 4.1	Plot of Shale Transit Time Versus Depth of Burial	65
Figure 5.1	Changing Pore Fluid Chemistry During Mesodiagenesis	76
Figure 5.2	Textural States of Mesodiagenetic Porosity	79

LIST OF PHOTOS

	Page	
Photo 3.1	Thin section photograph showing quartz rich nature of Niton Basal Quartz sandstone	31
Photo 3.2	Dissolution of calcite resulting in formation of secondary porosity	31
Photo 3.3	Secondary porosity produced by dissolution of soluble carbonate mineral	33
Photo 3.4	Oblong pore of secondary origin	33
Photo 3.5	Detrital illite clay matrix situated between detrital quartz grain contacts	42
Photo 3.6	Quartz grains "floating" within illitic clay matrix that was concentrated by activity of burrowing organisms	42
Photo 3.7	Pore lining authigenic illite (I) and pore filling authigenic kaolinite (K)	44
Photo 3.8	Birefringent pore lining authigenic illite	44
Photo 3.9	Short digitate lath-like extensions of authigenic illite	45
Photo 3.10	Location of previous photograph	45
Photo 3.11	Authigenic quartz overgrowth covered by authigenic, pore rimming illite	46
Photo 3.12	Authigenic quartz overgrowth just beginning to be covered by authigenic illite	46
Photo 3.13	Authigenic illite bridging pore throat between two quartz grains	48
Photo 3.14	Close-up view of pore-bridging authigenic illite	48

		Page
Photo 3.15	Possible authigenic illite between detrital grains	49
Photo 3.16	Possible authigenic illite between detrital grains	49
Photo 3.17	"Stacked booklets" of pore filling authigenic kaolinite	50
Photo 3.18	"Stacked booklets" of pore filling authigenic kaolinite. Crossed polars.	50
Photo 3.19	Progressive authigenic mineral assemblage (quartz, illite, kaolinite)	51
Photo 3.20	Progressive authigenic mineral assemblage (quartz, illite, kaolinite)	51
Photo 3.21	Stacked booklet morphology of authigenic kaolinite	53
Photo 3.22	Progressive authigenic mineral assemblage viewed in S.E.M.	54
Photo 3.23	Progressive authigenic mineral assemblage viewed in S.E.M.	54

LIST OF TABLES

	Page
Table 2.1A Type of Production for Niton Basal Quartz "B" Pool	12
Table 2.1B Original HydroCarbon-in-Place For Entire Niton Basal Quartz "B" Pool	13
Table 3.1 Point Count Data	28

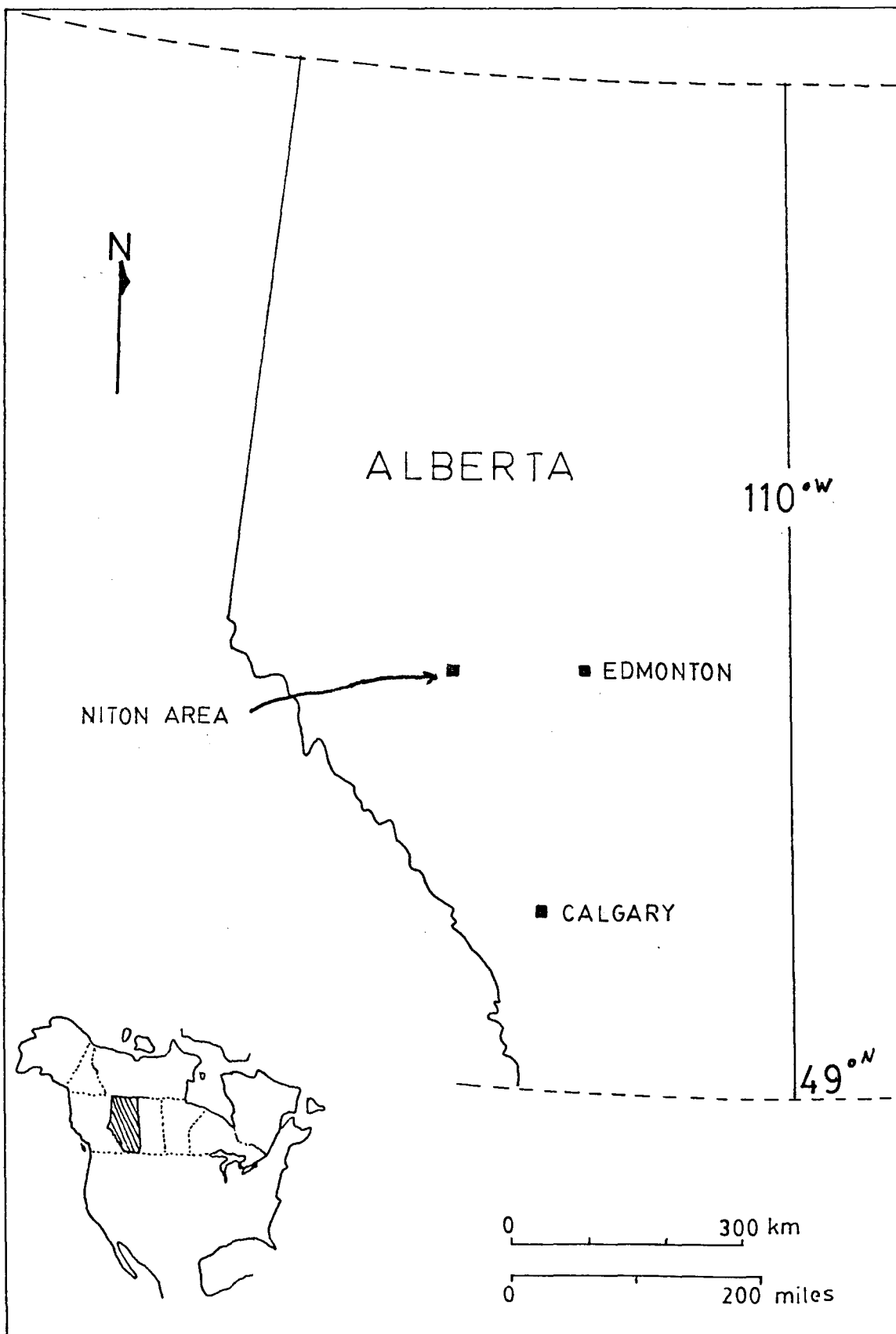
CHAPTER 1

AREA OF STUDY AND STATEMENT OF PROBLEM

The Lower Cretaceous, Niton Basal Quartz hydrocarbon reservoir, located approximately 160 kilometres west of Edmonton, Alberta, was discovered by Imperial Oil Limited in 1965. The Niton pool is bounded by townships 54 to 56, ranges 11 to 13, west of the fifth meridian, (Figure 1.1). The average thickness of the major producing zone for the entire pool is 5.3 metres, (17.7 feet). The subsurface depth of the Basal Quartz sandstones examined in this paper range from approximately 1910 metres to 2010 metres, (6367 to 6700 feet). The Niton Basal Quartz "B" pool, dipping approximately 11.2 metres per kilometre in a south-west direction, has formed as a result of a stratigraphic pinchout of updip porosity. The downdip boundary of the pool is defined by the presence of water saturated sands.

Construction of several cross sections through the Niton Basal Quartz interval has revealed a complex pattern of reservoir sands. The sands have been divided into a sequence of four zones by the Esso Research staff. These zones were designated A, B, C, D in descending stratigraphic order. The B, C, D zones have been grouped together into the Niton Basal Quartz "B" pool and it is these sands which are the primary subject of the present study.

The Esso Research staff noted that at some places within



the Niton Basal Quartz "B" pool there were localized areas of increased clay accumulation lowering the reservoir potential of the Basal Quartz sands. One hypothesis is that some of these damaging clays were of secondary (authigenic) origin, however, the presence of a significant amount of primary (detrital) clay was also anticipated.

The proportion and type of primary clay minerals is to a large extent controlled by the original environment of deposition of the sediment, whereas the varieties and relative abundances of authigenic clay minerals is heavily dependent upon secondary diagenetic processes. These diagenetic processes may or may not be related to the environment of deposition.

Cores from three wells penetrating the Niton Basal Quartz "B" pool were logged in detail by the present author with the purpose of determining the depositional environment of the Niton Basal Quartz sandstones. Shales and sands from these cored wells were sampled to provide materials for laboratory studies. The purpose of these studies was:

- i) to determine what type and proportion of the clay minerals are diagenetic in origin;
- ii) to observe vertical and lateral variations of both detrital and authigenic clays;
- iii) to help determine the provenance of the sediment through analysis of the clay mineralogy.

GENERAL STRATIGRAPHY

Due to economic interest in the oil and gas reserves of the Lower Cretaceous strata of Alberta, numerous reports on the sub-surface stratigraphy and petrography of these rocks have been written. Works of immediate importance to this thesis include Glaister (1959), Williams (1963), Mellon (1967), and Bayliss and Levinson (1976).

In the Niton area the Lower Cretaceous (Lower Mannville) Basal Quartz (or Ellerslie) sands are Aptian and early Albian in age. These Lower Mannville sandstones are situated unconformably upon the Fernie Formation of Jurassic age. Glaister (1959) found the Basal Quartz sandstones of Central Alberta to be correlative with the Cutbank and Sunburst sandstones (Lower Blairmore) of Southern Alberta.

The Lower Mannville, Basal Quartz sandstones are generally medium to fine grained orthoquartzites. The Basal Quartz member is overlain by the fossiliferous "Calcareous" member. The division between the Lower and Upper Mannville members is placed at the top of the "Calcareous" member, (Glaister, 1959). The Upper Mannville sandstones are distinguished from the Basal Quartz sands by the substantially increased abundances of feldspar and rock fragments in the Upper Mannville sands, (Williams, 1963).

Correlation between Mannville sediments and other stratigraphic units in southern Alberta have been given by

Glaister (1959) and by Williams (1963). The stratigraphic nomenclature followed in this report is presented in Figure 1.2.

DEPOSITIONAL FRAMEWORK, REGIONAL AND LOCAL

Regional:

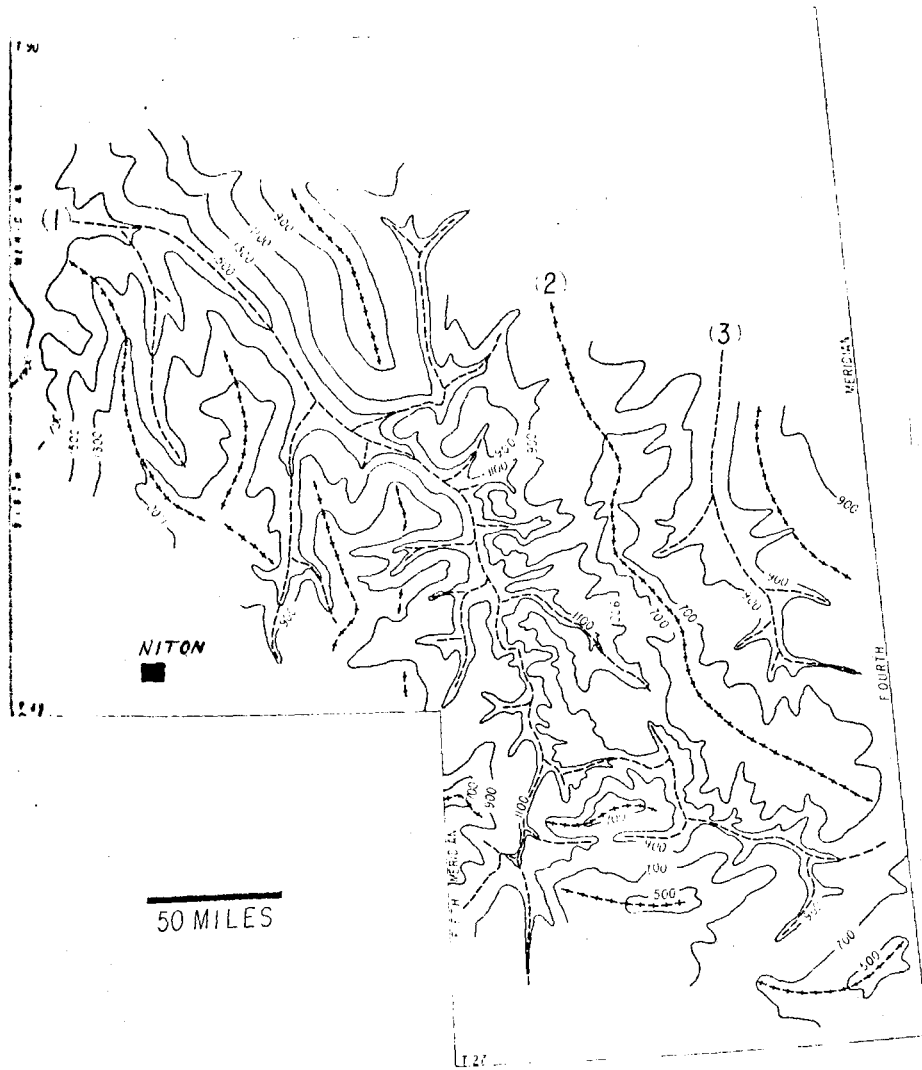
In the Late Jurassic history of Western Canada the intrusion of the Nelson and Cassiar-Omenica batholiths within the Western Cordillera was followed by considerable uplift and erosion. As uplift continued into the early Cretaceous, erosion of the highlands provided a westerly source of sediment to the Central Alberta area, (Jardine, 1974). Through petrologic studies, the Canadian Shield to the east has also been recognized as a source region of detrital sediment to the Central Alberta area, (Glaister, 1959).

The considerable relief upon the sub-Cretaceous erosional surface, averaging 90 to 120 metres, (300 to 400 feet), significantly influenced the distribution of the Lower Mannville sediments, (Figure 1.3). Deposition of the earliest Mannville sediments, in a dominantly fluvial environment, resulted in an infilling of the topographic lows (valleys) of the sub-Mannville surface. Further sediment deposition resulted in a "smoothing out" effect of the irregular erosional surface. Hence the thickest Lower Mannville deposits occur in conjunction with sub-Mannville surface lows, whereas thin deposits correspond

PERIOD	EUROPEAN STAGE	GROUP	NITON AREA
LOWER CRETACEOUS	ALBIAN	UPPER MANNVILLE	
			GLAUCONITIC S.S.
	APTIAN	LOWER MANNVILLE	CALCAREOUS MEMBER
			BASAL QUARTZ S.S. or ELLERSLIE S.S.
UNDERLYING STRATA			 JURASSIC FERNIE FORMATION

(After Glaister, 1959)

FIGURE 1.2



Isopach of Lower Cretaceous strata
in Central Alberta.

(After Williams, 1963)

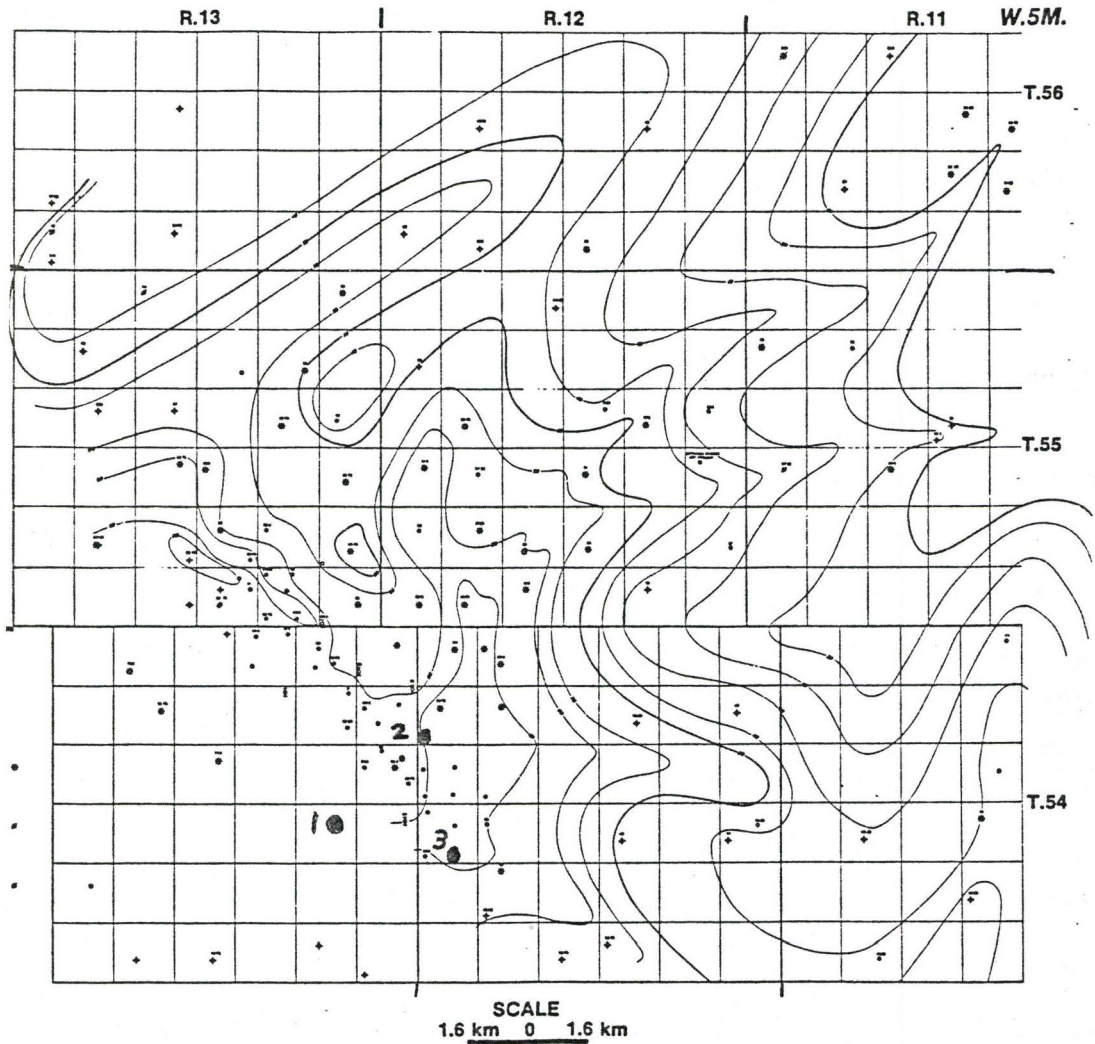
FIGURE 1.3

with deposition above resistant topographic ridges on the sub-Mannville erosional surface, (Williams, 1963), (Jardine, 1974).

At the close of the Lower Mannville, the early Cretaceous sea in Northern Alberta transgressed southward replacing the dominantly continental to deltaic environments of Central Alberta with marine sedimentation. Further subsidence at the end of Mannville times resulted in further transgression of the Arctic sea until it coalesced with the Southern Gulfian sea, (Jardine, 1979). The appearance of shallow marine to continental deposits late in the Cretaceous marked a period of emergence and subsequent erosion.

Local Depositional Framework:

In the Niton area the Lower Mannville Basal Quartz (or Ellerslie) sands were deposited over the Jurassic Fernie Formation. The Jurassic erosional surface in this area consisted of a series of northeast-southwest trending topographic ridges and valleys, (Figure 1.4). Deposition of the earliest C and D sand zones of the Niton Basal Quartz "B" pool resulted in a smoothing out of the irregular unconformity surface. As a consequence of the C and D sands infilling topographic lows, they often possess poor lateral continuity, (ie. discontinuous between wells located 1 to 2 km apart),



Niton Basal Quartz "B" Pool Isopach Map

Well Locations

- 1: 10-14-54-13w5
- 2: 4-30-54-12w5
- 3: 2-18-54-12w5

(From Niton Basal Quartz
"B" Pool Reserves Study
IPRC-19ME-79)

FIGURE 1.4

compared with the more laterally extensive B zone sands deposited on the less irregular surface above them.

Nonetheless, the B zone sands still do exhibit some controlling influence by the unconformity surface beneath.

CHAPTER 2LOCAL STRATIGRAPHY AND FACIES DESCRIPTIONIntroduction:

Comparison of the Niton Lower Mannville sediments and facies with known modern sedimentary facies should allow one to reconstruct the environment of deposition of the Niton Lower Mannville sediments. Therefore cores from 3 wells penetrating the Basal Quartz sandstones were logged and sampled in order to determine the depositional facies.

The 3 wells, located about 3.2 kilometres from each other and situated in the southern portion of the Niton field, were:

- i) 2-18-54-12W5 , an oil well
- ii) 4-30-54-12W5 , a gas well
- iii) 10-14-54-13W5 , a water disposal well.

From this point on, the wells will be referenced only by the first two digits of their location numbers. (Example; 2-18-54-12W5 = 2-18)

The Basal Quartz sands of well 10-14 are situated within the downdip aquifer on the south-west side of Niton pool and consequently contain no hydrocarbons. The producing Basal Quartz sandstones of wells 4-30 and 2-18 are located updip of well 10-14, above the oil water contact.

Of the three zones of Basal Quartz sandstones within the Niton Basal Quartz "B" pool the B zone sand is the most important. It contains the bulk of hydrocarbon reserves, because of its wider lateral distribution relative to the less continuous C and D zone sands stratigraphically beneath. Although hydrocarbons may be present within the A zone sands there is no production from these sands. Table 2-1 A presents a summary of the type of production from each zone of the three wells studies; Table 2-1 B lists the original hydrocarbons-in-place for the entire Niton Basal Quartz "B" pool as calculated by Esso Resources.

TABLE 2-1 A

TYPE OF PRODUCTION FOR NITON BASAL QUARTZ "B" POOL

	10-14-54-13W5	4-30-54-12W5	2-18-54-12W5
B Zone	Water Disposal	Gas	Oil
C Zone	Water Disposal	Gas	No pay assigned
D Zone	No pay assigned	Gas	No pay assigned

TABLE 2-1 B

ORIGINAL HYDROCARBON-IN-PLACE FOR ENTIRE
NITON BASAL QUARTZ "B" POOL

	Oil-in-Place	Gas-in-Place
B Zone	8,744x10 ³ m ³	11,045x10 ⁶ m ³
C Zone	760x10 ³ m ³	1,424x10 ⁶ m ³
D Zone	2,625.1x10 ³ m ³	1,449x10 ⁶ m ³

From Table 5 Niton Basal Quartz
"B" Pool Reserves Study
IPRC-19ME-79

FACIES DESCRIPTIONS

Introduction:

Within the Niton Lower Mannville sediments 6 facies have been recognized and defined. Characteristics used in the definition of the facies were; rock composition, grain size, primary sedimentary structures and degree of bioturbation. Figures 2.1, 2.2, 2.3 show the locations of these facies.

Laminated Mudstone/Siltstone Facies, (L.M.S.):

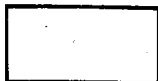
This facies was characterized by thin alternating beds (millimetre to centimetre scale) of black shales with silt (or sand). The relative proportions of silt (or sand) to shale varies from approximately 20 percent silt (80 percent shale) to about 60 percent silt (40 percent shale). Mud

LEGEND FOR FIGURES 2.1, 2.2, 2.3

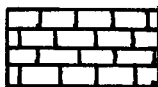
LITHOLOGY



MUDSTONE



SANDSTONE



FOSSILIFEROUS DEBRIS (COQUINOID FACIES)



COAL HORIZON

BIOTURBATION AND SEDIMENTARY STRUCTURES



TROUGH CROSS BEDDING



CURRENT RIPPLE



WAVE RIPPLE



MUD FLAZER (FLAZER BEDDING)

MUDSTONE EXHIBITING LENTICULAR/
WAVY BEDDING

STYLOLITE



RIP-UP CLASTS



WEAKLY BIOTURBATED



MODERATELY BIOTURBATED



STRONGLY BIOTURBATED (CHURNED)

10-14-54-13W5

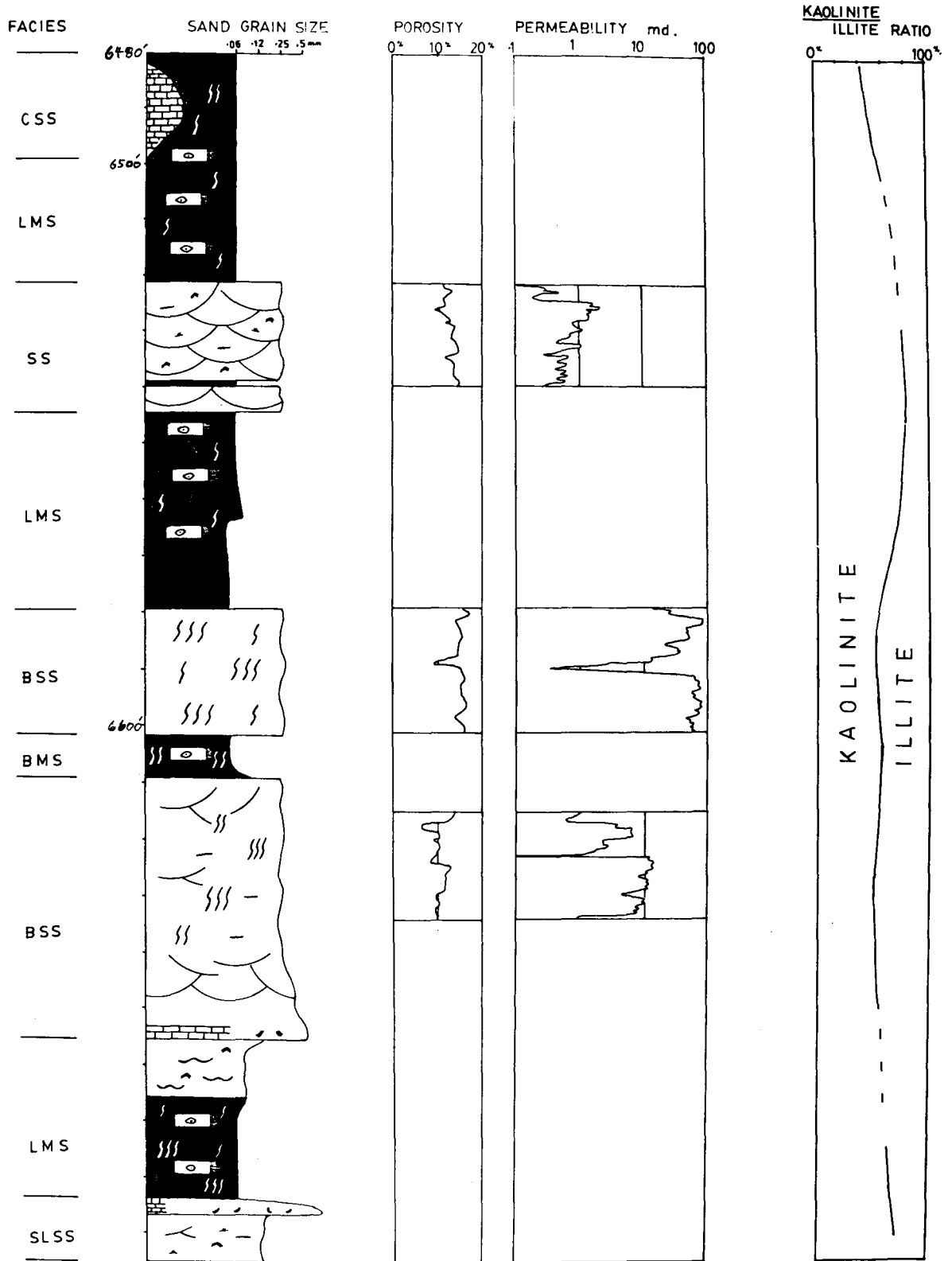


FIGURE 2.1

4-30-54-12W5

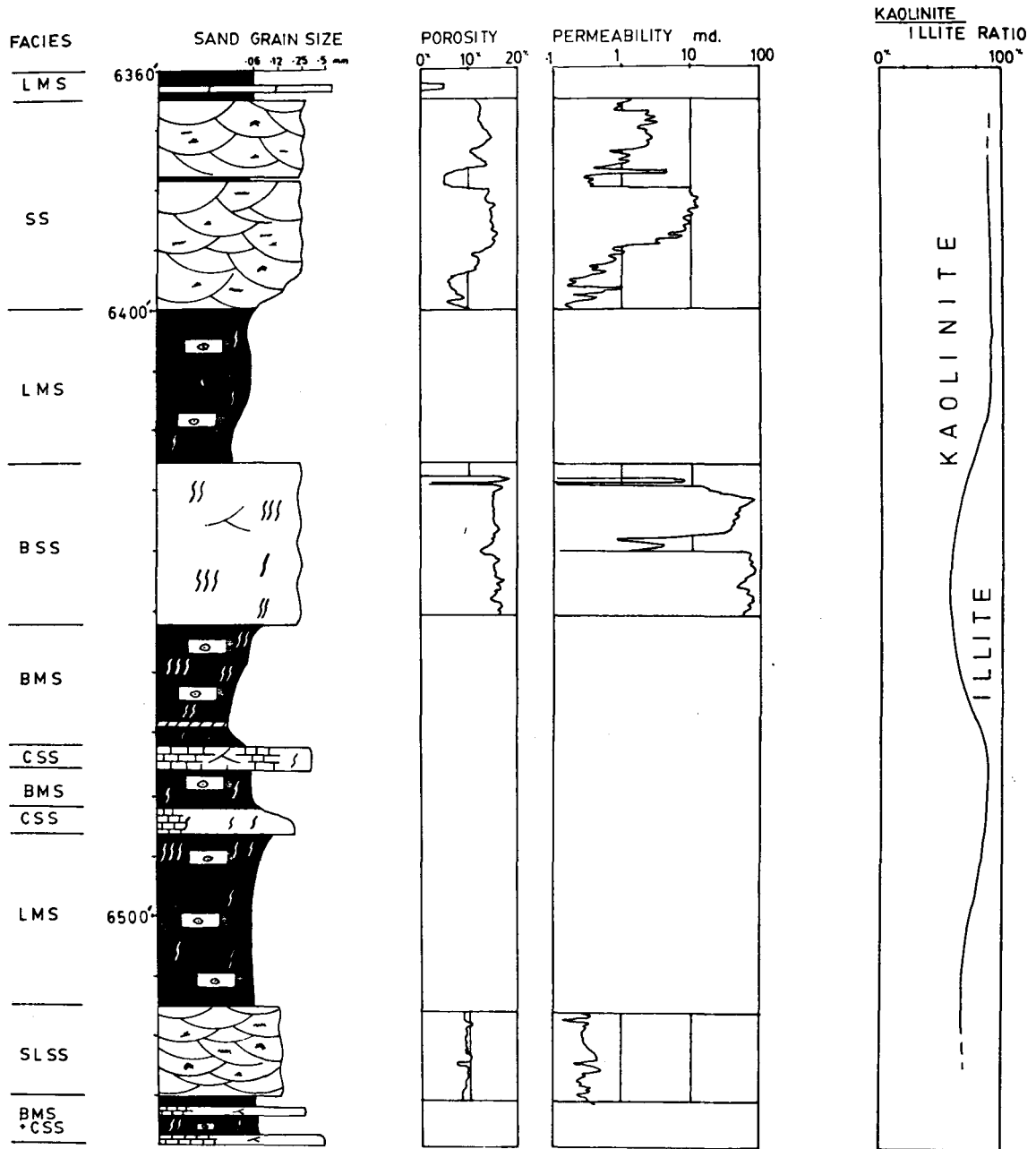


FIGURE 2.2

2-18-54-12W5

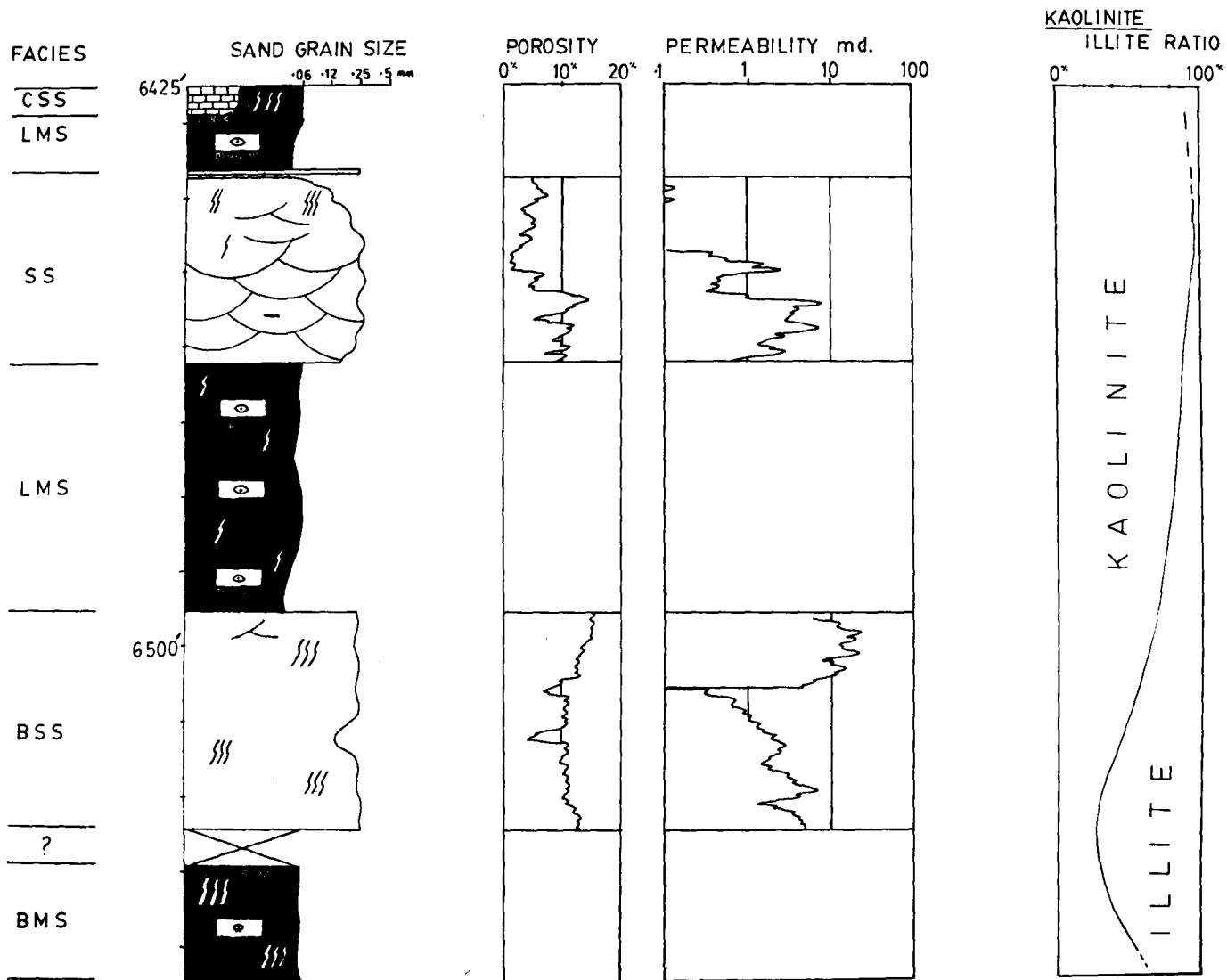


FIGURE 2.3

rich zones contain horizontally running lenses of silt. These lenses are isolated from other lenses both in a horizontal and vertical direction. This structure is called (single) lenticular bedding, (Reineck and Singh, 1973). As the percentage of silt (or sand) increases the isolated lenses gradually become connected in a horizontal direction, many forming into continuous wavy beds of silt (or sand), interbedded with thin shale beds. This structure is called wavy bedding, (Reineck and Singh, 1973).

In one instance (well 10-14 at 6660 feet) the proportion of silt in this facies has increased to about 80 percent. Mud streaks (flazers) have been preserved in troughs of ripples within the silt/sandstone. Reineck and Singh (1973) call this structure flazer bedding.

Within the silt (or sand) lenses of this facies both wave and current ripple foresets were visible. Many horizontal burrows were present within the shale beds. In addition, glauconite and pyrite were present in varying amounts and traces of siderite were observed within the 10-14 well, (6579 feet). In two instances (well 4-30, 6363 feet) (well 2-18, 6437 feet) the laminated mudstone/siltstone facies is interrupted by a 0.3 metre (1 foot) thick layer of medium to coarse grained, poorly sorted grey sandstone. Shell fragments may be present where this facies is transitional to the coquinooid sandstone facies.

Bioturbated Mudstone/Siltstone Facies (B.M.S.):

This facies is very similiar to the laminated mudstone/siltstone facies however, the churning action of burrowing organisms has almost completely destroyed the lenticular and wavy structures that once existed. Burrows are predominantly horizontal although vertical burrows are present in many cases. A thin 10 centimetre (4 inch) coal seam is interbedded with this facies in well 4-30. The laminated mudstone/siltstone facies may grade over a distance of several centimetres into the bioturbated mudstone/siltstone facies, or the two facies may be separated by one of the Basal Quartz sandstone zones.

Sandstone Facies (S.S.):

This facies was composed of fine to medium grained, speckled, quartz rich sandstones, cream to light brown in colour. Only the three A Zone sands were included within the sandstone facies. The cream coloured portions of sandstone were due to the large abundances of light coloured intergranular clay. As anticipated core plug measurements showed the clay rich sands to possess lower than average porosities. Average porosities for the 3 A Zone sands ranged from about 7 percent to 14 percent and average permeabilities varied from roughly 0.8 millidarcies (md) to 8 md.

Small scale bidirectional ripples were present in the cored sands. In most cases these ripples were defined by the

presence of paper thin shale laminations. High angle (15-35°) parallel sand laminae, often exhibiting truncations were also visible in the core. These were interpreted to be large scale trough crossbeds. In a few instances scour and fill structures were also visible.

With the aid of a binocular petrographic microscope the sandstones of this facies were found to contain well sorted, subangular to subrounded quartz grains. Some of the low porosity clay-bound sandstones exhibited only moderate sorting. Clay-rich sands generally were more friable than the relatively clay-free sands.

The absence of bioturbation was common to all three of the A Zone sands examined, although several vertical burrows were found in conjunction with shale breaks in the top of the 2-18 well A Zone sand. Pyrite, along with minor amounts of glauconite were present. Pyrite occurrences were in most cases confined to shale breaks and burrow traces.

Bioturbated Sandstone Facies (B.S.S.):

The sandstones of this facies consisted of bioturbated, fine to medium grained, quartz rich, glauconitic sands. All three of the B Zone sandstones, as well as the C Zone of well 10-14 belonged to this facies. The C Zone sand contained a smaller amount of glauconite compared to the B Zone sands. These speckled (or more rarely mottled) sandstones were light

grey to light brown in colour. Sands of this facies observed in well core varied in thickness from approximately 6 m (20') to 12.6 m (42'). Average porosities ranged from approximately 10 percent to 15 percent; average permeabilities varied from about 7 md to 60 md.

Extensive churning of the sediment by burrowing organisms has destroyed most of the primary sedimentary structures. However, certain portions of the sediment, which apparently experienced a lesser intensity of bioturbation, occasionally exhibit inclined (10-20°) parallel laminae defined by undisturbed paper thin shale laminations.

Examination of core samples with the petrographic microscope showed the quartz-rich sediment to be subangular to subrounded and moderately sorted to well sorted. Glauconite present within the sandstones showed no quantitative trends, except that the B Zone sand in well 10-14 exhibited a noticeable decrease in abundance of glauconite proceeding stratigraphically upwards within the sand. Pyrite occurrences were generally confined to burrow traces. Rare pyrite concretions (diagenetic features) were found cementing together several quartz grains within the sediment. Some carbonaceous lamellae were observed, and a single vertical root trace was tentatively identified. The base of the C Zone sandstone in the 10-14 well was floored by a 0.6 m (2') thick fossiliferous sandstone.

Silty Sandstone Facies (S.L.S.S.):

The D Zone sandstones were the exclusive members of this facies. These quartz-rich sandstones were white coloured, very fine to fine grained and were approximately 4.5 m (15') in thickness. The average porosity of the 4-30 well D Zone was about 9 percent; average permeability was roughly 0.5 md.

Due to the absence of bioturbation within this facies, paper thin shale laminations were preserved and defined abundant low angle (5 to 10°) laminae, and wave and current ripples. The D Zone sands were generally well sorted, sub-angular to subrounded. Moderate amounts of pyrite and glauconite were present, and many small stylolites were visible in the core. Above the D Zone in well 10-14 was a 0.5 m conglomeratic bed containing many shell fragments and rip-up clasts of shale and sandstone.

Coquinoid Sandstone Facies (C.S.S.):

Several occurrences of the coquinoid sandstone facies were present within the Lower Mannville (Basal Quartz) sediments. The 2.4 metre (8 foot) thick C Zone of well 4-30 was also a member of this facies. The coquinoid sandstone facies consisted of bioturbated muds, silts and sands mixed with varying proportions (10 percent to 75 percent) of coarse to conglomeratic, randomly oriented, broken bivalve shell fragments. Rare fragments of gastropod shells were found.

Members of this facies examined in core varied from 0.3 m (1') to 4.8 m (16') in thickness. Contacts of this facies with adjacent facies were either gradual (eg. contact with L.M.S. facies in well 2-18 at 6430 feet), or sharp, (eg. sharp contact with B.M.S. facies in well 4-30 at 6472 feet). Pyrite was present within this facies, and oil staining was visible within the more arenaceous portions of the 4-30 well C Zone.

INTERPRETATIONS

The Niton Basal Quartz "B" Pool Reserves Study (1979) by Esso Resources states that the Basal Quartz sandstones of the Niton area were deposited in an early Cretaceous fluvio-deltaic system. Because of the limited distribution of the C and D sand zones Esso Resources suggested that they were deposited in a fluvial system. Workers at Esso also stated that the depositional features of the non-reservoir C and D sediments, lenticular and wavy bedding (facies L.M.S. and B.M.S.) were characteristic of tidal flat or inter-distributary portions of a deltaic environment.

Concerning the B Zone sands, the Esso report stated that the greater vertical and horizontal continuity of the B Zone sands, the presence of glauconite and the extensive bioturbation of the sands infers deposition in a nearshore marine environment.

Although only 3 wells located within a limited area of the Niton pool have been examined, the observations by the

present author confirm, in part, the conclusions of Esso Resources concerning the depositional environment of the Niton Basal Quartz sediments.

The formation of lenticular, wavy and flaser bedding requires an environment in which deposition of ripples, by current or wave action, is followed by a period of slack water in which mud is deposited. Subtidal and intertidal environments are best suited for the formation of a continuum of lenticular to flaser bedded structures, (Reineck and Singh, 1973), (Blatt et. al, 1980). Consequently both the laminated mudstone/siltstone (L.M.S.) facies and the bioturbated mudstone-siltstone facies have been interpreted as forming within an inter-distributary tidal flat environment.

The C and D Zone sands, (B.S.S. and S.L.S.S. facies respectively) are surrounded in vertical succession by the interdistributary sediments of facies L.M.S. and B.M.S. According to "Walther's Rule of Succession of Facies" the C,D Zone sandstones and the interdistributary facies were at some time formed beside each other, (Walther in Blatt et. al, 1980). During the transgression of the early Cretaceous sea, the NE-SW trending ridges and valleys of the Jurassic erosional surface caused a serrated coastline to be formed in the Niton area, (Chapter 1). The D Zone sands may have been early (distributary) channels draining across the young upper deltaic deposits forming within the low lying topographic valleys. The poor lateral continuity of these sands would be due to their location

within the confines of the valleys, and the distributary channels in this case could develop beside the intertidal facies as observed.

For these distributary sands to have formed within a deltaic environment rather than under fluvial conditions would require the transgression of the early Cretaceous sea to have been further inland at this stage than is supposed by those suggesting a fluvial deposition of the lowermost (C, D sand zones) of the Niton Basal Quartz sands.

The C Zone sandstone of well 10-14 (facies B.S.S.) has been interpreted by the present author as a distributary channel deposit. The fossiliferous base of this sand is interpreted as a channel lag deposit. The remaining fine grained, glauconitic B Zone sands of the bioturbated sandstone facies (B.S.S.) may also represent distributary channel deposits.

The absence of bioturbation, in association with large scale cross bedding and wave and current ripples suggests that the sandstone facies may be distributary mouth bar deposits, (Weimer, 1978), (Reineck and Singh, 1973). The thin coal horizon above the A Zone sand in well 2-18 probably represents organic debris brought in by flood stage waters.

Coquinoid facies exhibiting sharp bottom contacts with adjacent facies, (L.M.S. or B.M.S. facies), have been interpreted as storm deposits of shell debris washed from interdistributary bays or lagoons up onto marshy interdistributary

mud flats. Coquinoid facies with gradational contacts are probably "in situ" lagoonal or bay deposits that have been moderately reworked by wave and tidal action.

Examination and interpretation of the various facies within the Niton Lower Mannville sediments has led the author to the conclusion that deposition was within a complex deltaic environment. The elongate early Cretaceous sea may have provided sufficient tidal activity to significantly affect the morphology of this delta. A tidally influenced delta is also inferred by the abundance of wavy to lenticular bedding which are common features in macrotidal deltaic deposits.

CHAPTER 3PETROGRAPHIC OBSERVATIONSTHIN SECTION OBSERVATIONSIntroduction:

A total of 16 thin sections were prepared from 45 samples collected from facies S.S., B.S.S., S.L.S.S. and C.S.S. of the Niton Basal Quartz sandstones. Table 3.1 contains a listing of the samples taken, their stratigraphic depth, and the facies from which they were obtained. Petrographic compositions and porosities of each thin section were determined by microscopic examination of a minimum of 250 points on each thin section. For an average quartz composition of 77 percent, using a minimum of 250 point counts, the confidence limit would be approximately 6 percent if sampling was repeated, (Pettijohn et al, 1972).

Composition:

Minerals identified in the Basal Quartz sandstones were: quartz, chert, mica, rock fragments, calcite, dolomite, feldspar, pyrite, glauconite, clay matrix (detrital illite and kaolinite), and clay cement (authigenic illite and kaolinite). The bulk of the porosity was primary in origin, however, several pores of secondary origin were also observed. Quartz (69 percent - 89 percent) and clay minerals (2 percent - 24 percent) were the major constituents. Detrital feldspars were rare (zero -

TABLE 3-1

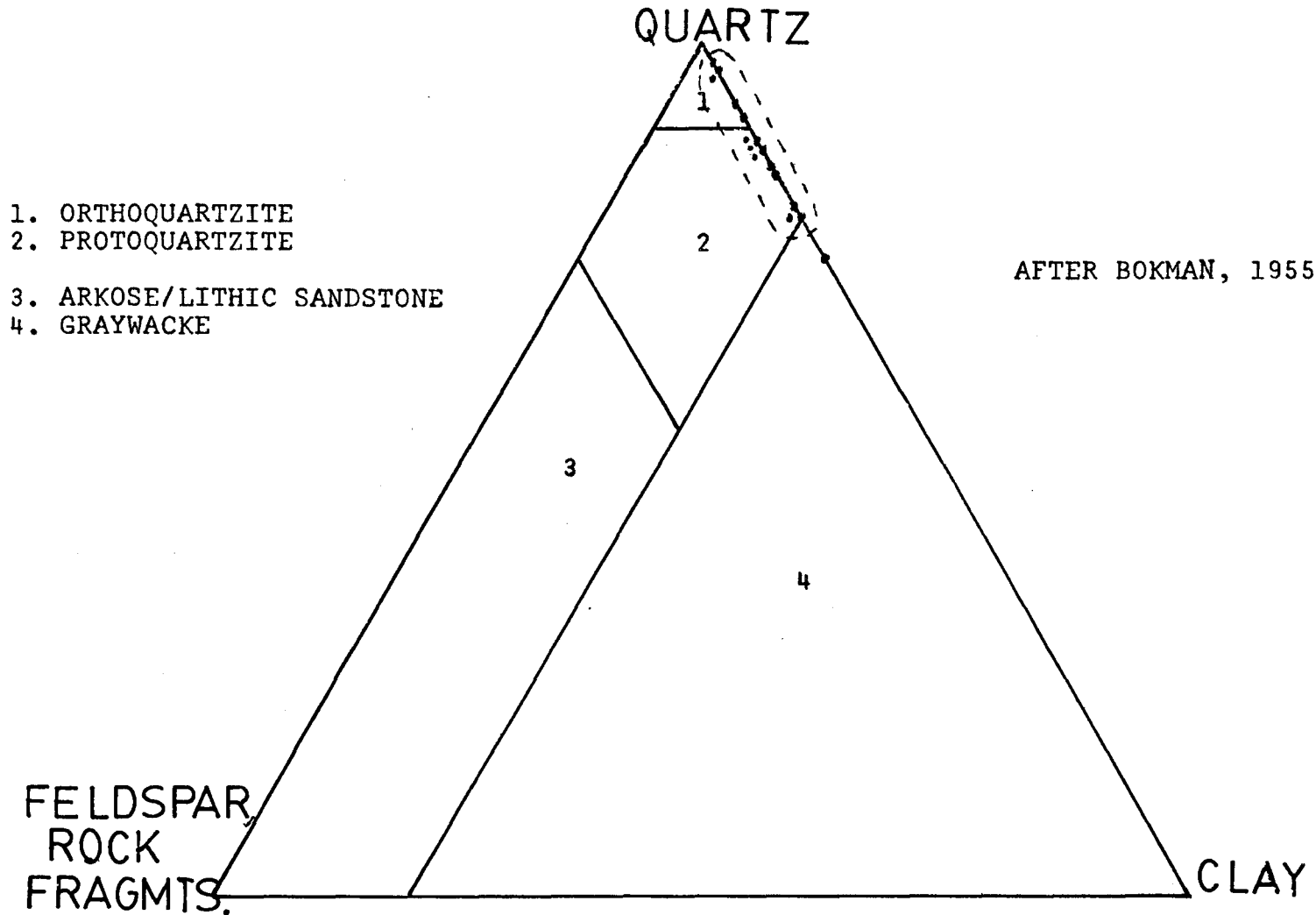
FACIES	SAMPLE NUMBER	DEPTH	QUARTZ	CHERT	CLAY	GLAUCONITE	OPAQUES	HEAVY MINERALS	FELDSPAR	POROSITY	CALCIUM CARBONATE	FRAGMENTS	TOTAL
SANDSTONE FACIES	2-18-5	6445'	73.7	10.6	14.1	---	---	1.3	--	---	---	---	99.7
	2-18-6	6453'	76.6	---	14.5	---	2.4	.4	--	6	---	---	99.9
	4-30-4	6385'	81.5	1.6	9.9	---	---	1.2	--	4.9	.8	---	99.9
	4-30-5	6394'	69.1	5.1	16.5	---	8.1	1.1	--	---	---	---	99.9
	10-14-3	6525'	81.1	---	6.1	1.8	1.4	---	--	8.9	1.1	---	100.4
BIOTURBATED SANDSTONE FACIES	2-18-9	6500'	80.1	.3	7.3	2.8	1	---	--	7	1	1	100.5
	2-18-11	6516'	81.2	.5	8.9	5.1	.8	---	--	2.4	1.1	---	100
	4-30-7	6430'	72.3	.4	14.4	2.5	3.2	---	--	5.8	.7	.7	100
	4-30-8	6443'	76.4	---	3.6	6.5	.4	.4	--	12.4	.4	---	100.1
	10-14-8	6580'	77.2	---	8.2	3.0	---	---	--	9.7	1.1	.7	99.9
	10-14-9	6588'	83.3	---	7.1	2.0	1.0	---	--	5.4	.3	.7	99.8
	10-14-11	6616'	71.7	---	23.9	.4	2.9	---	--	1.1	---	---	100
	10-14-12	6619'	88.5	---	1.5	---	.7	---	--	8.9	.4	---	100
SILTY SANDSTONE	4-30-15	6519'	85.3	---	2.8	---	.6	.3	.8	4.5	5.6	---	99.9
	10-14-18	6692'	81.2	---	2.4	---	.7	.7	.3	2.1	12.5	---	99.9
COQUINOID FACIES	4-30-13	6488'	78.2	---	5.2	.4	1.8	---	---	4.4	10.0	---	100

one percent) within the Niton Lower Mannville sediments. These findings are in agreement with the results of Bayliss and Levinson (1976), Glaister (1957), Mellon (1967), and Williams (1963). According to the classification scheme of Bokman (1955) all but one of the sandstones samples were classified as protoquartzites or orthoquartzites, (Figure 3.1) (Photo 3.1).

Quartz Grains: The majority of quartz grains within the Niton Basal Quartz sandstones were monocrystalline (approximately 1 percent were polycrystalline). Roughly 40 percent of the grains exhibited little or no strained extinction, and most quartz grains possessed authigenic quartz overgrowths. Quartz grains were subangular to subrounded and ranged in size from 3.5 ϕ (.088 mm) to 1 ϕ (0.5 mm). The quartz of the bottom-most sandstones (D Zone, Facies S.L.S.S.) were the finest grained, the uppermost "sandstone" facies were the coarsest. This coarsening upwards pattern is anticipated within a deltaic environment, (Reineck and Singh, 1973).

The finer sized quartz grains were subangular in comparison with the coarser, subrounded grains. During transport the finer grained sand sediment was probably carried in suspension rather than as bed load, consequently the finer grains were subject to less abrasion (and less rounding) than the coarser grained bed load, (G.V. Middleton, Personal Communication). In some instances the coarser grained quartz sands were subangular, rather than subrounded. Pseudo-angularity has been imparted to

FIGURE 3.1



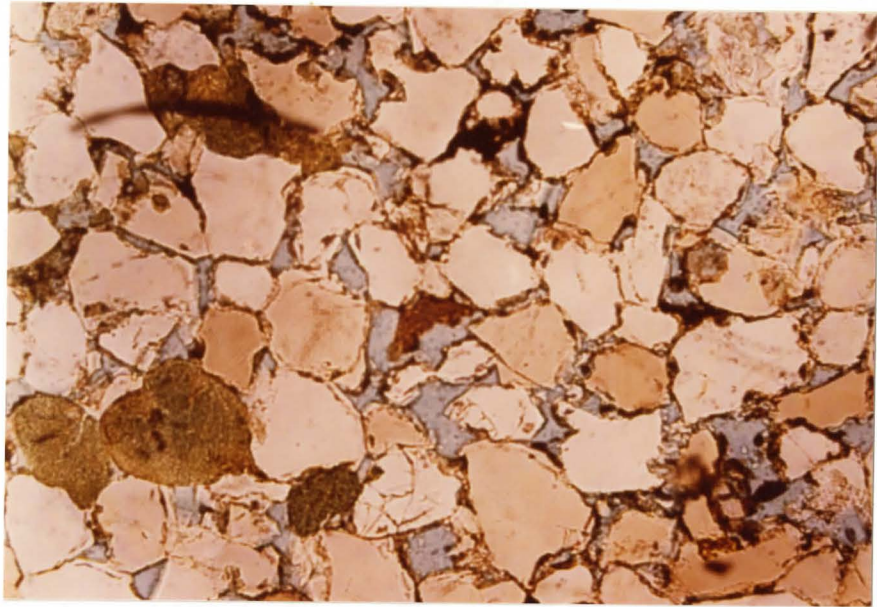


PHOTO 3.1 Thin section photograph showing quartz rich nature of Niton Basal Quartz sandstone. Pore spaces are filled with blue coloured epoxy. Sample 4-30-8, 63X magnification.

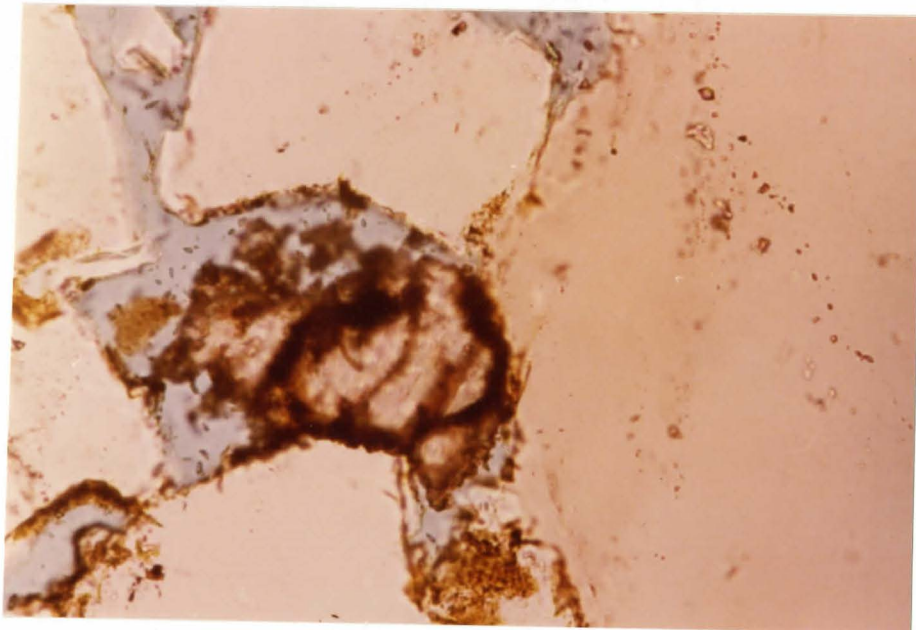


PHOTO 3.2 Dissolution of calcite resulting in formation of secondary porosity. Sample 4-30-8, 250X magnification.

the subrounded quartz grains by the angular crystal terminations of the quartz overgrowths, (Williams, 1963).

Inclusions of rutile and zircon were common in many quartz grains, and rare boehm lamellae were observed.

Calcite: Calcite was present as detrital shell fragments and more commonly as small patches of authigenic cement. In several instances calcite cement poikilotopically cemented several quartz grains. Both detrital and authigenic calcite were usually corroded, and in many cases dissolution of soluble carbonate minerals resulted in the development of secondary porosity, (Photos 3.2, 3.3). The greatest abundances of calcite were in the silty-sandstone facies (S.L.S.S.). The coquinoid sandstone facies contained many very fine grained euhedral to subhedral dolomite rhombs floating within the detrital clay matrix. In one instance calcite was observed totally replacing a plagioclase feldspar.

Feldspar: Highly corroded feldspars, tentatively identified as orthoclase feldspars, were present within the Basal Quartz sandstones. Dissolution of feldspars has in a few cases resulted in the development of secondary porosity, (Photo 3.4).

Glauconite: Detrital grains of glauconite, deformed during compaction, were recognized by their green colouring, high birefringence (often masked by the colouring of the mineral) and pellet-like morphology. Shrinkage features and dissolution/alteration features were observed in several cases.

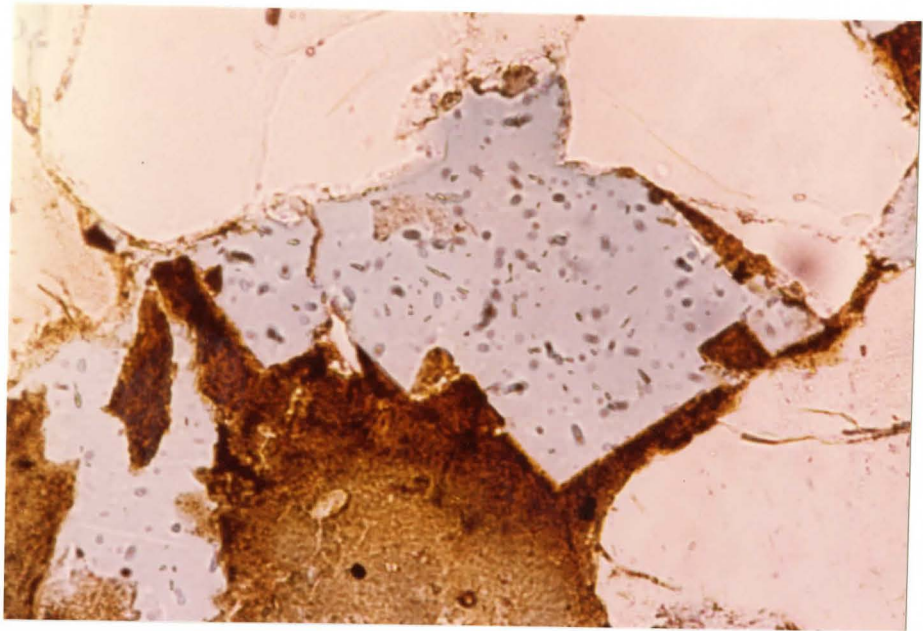


PHOTO 3.3 Secondary porosity produced by dissolution of soluble carbonate mineral. Sample 4-30-8, 250X magnification.

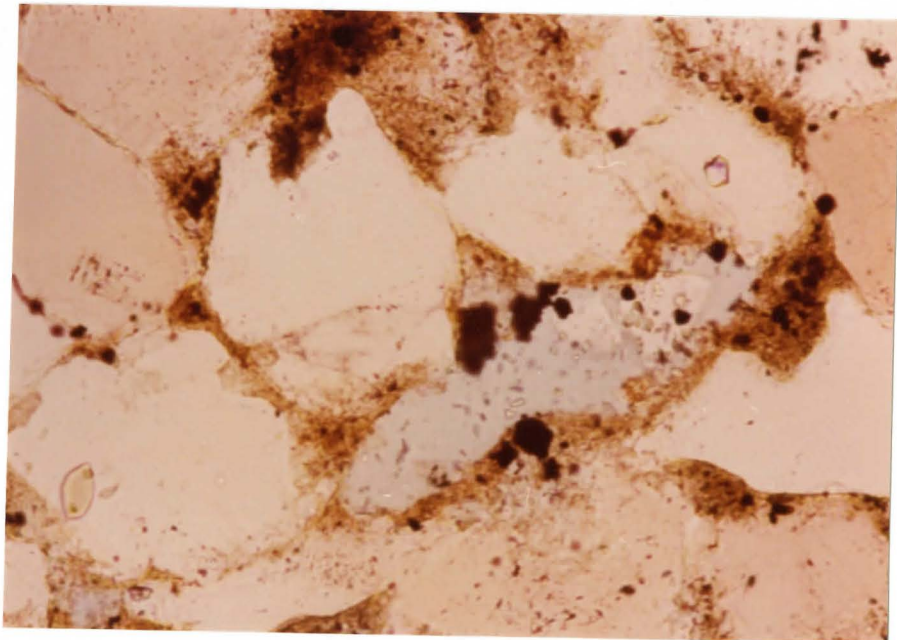


PHOTO 3.4 Oblong pore of secondary origin, possibly produced by the dissolution of detrital feldspar. 160X magnification.

Other Minerals: Detrital chert present within the Niton Basal Quartz sandstones was generally confined to the uppermost sandstone facies. Detrital mica flakes, deformed between quartz grains during compaction of the sediment, were observed in several instances. Pyrite occurred as medium sized subhedral to anhedral grains, and as very fine grained constituents present within portions of the clay matrix. Traces of echinoderm fragments, bivalve shell pieces and phosphatic oolites were also present in thin sections from the C.S.S. and B.S.S. facies.

In many thin sections pores contained dark brown to isotropic matter identified as pore lining and pore bridging oil residue and bitumen. Heavy minerals present included abundant, well rounded zircon, lesser quantities of rutile and tourmaline and highly corroded garnets. Heavy mineral concentrations were observed to occur in horizontal planes in a few cases.

Because clay minerals are suspected of significantly reducing porosity and permeability within the Niton Basal Quartz sandstones, (Chapter 1), the following discussion will deal at length with the identification and differentiation of clay minerals within the Basal Quartz sandstones.

CLAY MINERALOGY

Introduction:

In order to evaluate critically and interpret the relative effects of porosity and permeability reduction by the occurrence of clay minerals, and to determine the degree of diagenesis, it is essential to identify and distinguish between allogenic (detrital) clays and authigenic clay minerals present within the Basal Quartz sandstones. Clay compositions and identifications were best determined for this report by using X-ray diffraction techniques. However, differentiation between the authigenic and detrital clay fractions was based primarily on the morphological features and textural relationships observed in petrographic thin sections and scanning electron photomicrographs of reservoir sandstone samples.

X-Ray Diffraction:

Identification of Clay Minerals:

Extensive Sampling of the well cores provided 36 small hand samples of shale and sandstone from which 18 suitable clay samples were chosen and prepared into clay mounts. Unfortunately the technique used was unable to avoid the mixing of authigenic and detrital clay minerals, consequently the two types of clay cannot be separated on X-ray diffraction patterns.

Sample Preparation: Approximately 10 grams of each sample was gently ground with a mortar and pestle until a fine powder of disaggregated sediment was obtained. Prior to crushing, each sample was thoroughly washed with distilled water to remove any contaminating drilling muds emplaced during recovery of the core. Distilled water was added to the powder and additional separation of the sediment was accomplished by mixing this solution in a high-speed blender for five minutes. Immediately following disaggregation the solution was transferred into a one-litre graduated cylinder, diluted, and allowed to stand for 225 minutes. After the time had elapsed the upper 200 millilitres of suspension was siphoned off. According to Stoke's Law, the <2 micron sediment fraction would supposedly be present in the solution. If at any time during the 225 minute settling period the clay showed signs of flocculation, the water was decanted and fresh distilled water added.

Several millilitres of the clay rich solution were then vacuum filtered through a .45 micron circular filter pad leaving a thin residue of basally oriented clay minerals on the filter surface. The clay residue was subsequently applied to a glass slide by a pressure rolling process.

Two slides from each sample were prepared. After drying for a minimum of 24 hours, one slide was scanned over an interval of 4° to $40^{\circ} 2\theta$ at a scanning speed of $1^{\circ} 2\theta$ per minute using CuK_{α} radiation at 16 Ma, 30 kv. After preliminary diffraction peak identifications were made, one slide from each

sample was placed for 1 hour, at 65°C, on a porcelain plate within a dessicator containing ethylene glycol. Within 12 to 24 hours after removing from the glycol the slide was scanned over a suitable 2θ interval. The original untreated slide was subsequently heated for 1 hour at 550°C and scanned once again over a suitable 2θ range.

Kaolinite: Untreated clay samples scanned in the range 4° to $40^\circ 2\theta$ revealed sharp diffraction peaks at approximately $12.6^\circ 2\theta$ (7\AA), $25.2^\circ 2\theta$ (3.5\AA), $37.9^\circ 2\theta$ (2.4\AA). It was concluded that these diffraction peaks represent the 001, 002, 003 reflections of kaolinite after they were found to collapse to an amorphous meta-kaolin structure following heating for 1 hour at 550°C. As anticipated, glycolation did not affect the kaolinite reflections. The sharp nature of the diffraction peaks suggested the dominance of a well crystallized, highly ordered 1T polytype rather than the disordered 1Md polytype, (Figure 3.2).

A diffraction peak at approximately 7\AA (002 reflection) is also produced by chlorite, however, the possibility of the presence of chlorite was ruled out by the absence of the 14.2\AA (001) chlorite reflection and by the strong nature of the 2.4\AA (003) kaolinite peak. A chlorite peak is usually weak or absent at this spacing.

Illite: Illite was tentatively identified by the presence of a commonly broad, diffuse 10\AA ($8.8^\circ 2\theta$) basal reflection in the untreated clay samples. The presence of an intense

X-RAY DIFFRACTION PEAKS SAMPLE 4-30-4

K • KAOLINITE
I • ILLITE
Q • QUARTZ

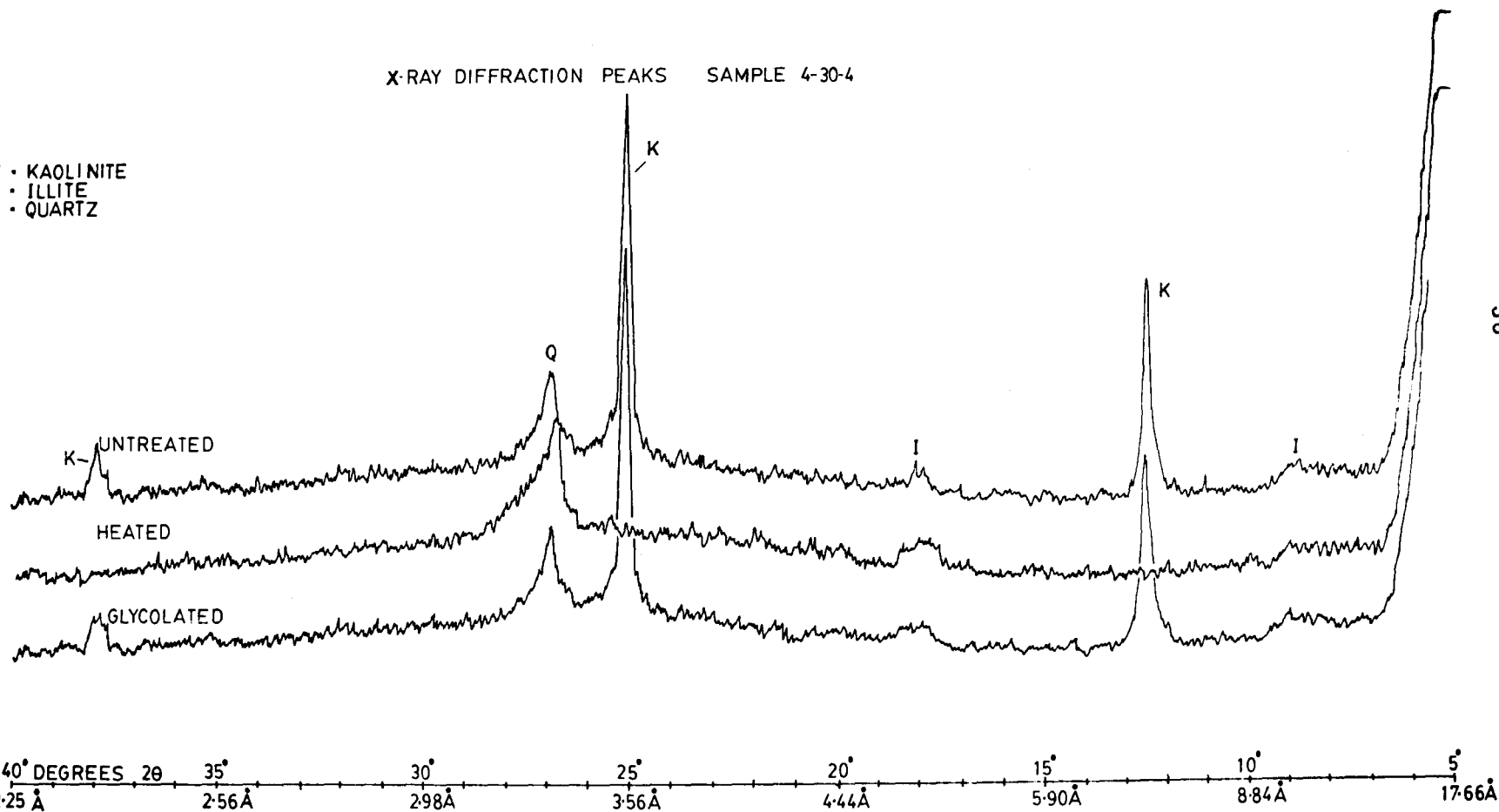


FIGURE 3.2

101 quartz reflection made it impossible to detect the $3.3\overset{\circ}{\text{Å}}$ illite reflection, although the $4.9\overset{\circ}{\text{Å}}$ illite reflection was evident. The broad, diffuse nature of the illite peak suggests either poor illite crystallinity (detrital 1Md polytype), or the existence of a mixed layer illite clay system. The rare occurrence of a sharp illite diffraction peak suggested the presence of a well crystallized (2M) polytype.

Confirmation of the tentative identification was made when the $10\overset{\circ}{\text{Å}}$ and $4.9\overset{\circ}{\text{Å}}$ diffraction peaks persisted after glycolation and heating of the clay samples, (Figure 3.2). The effect of heating to 550°C resulted in an occasional minor decrease of peak intensity which occurred due to a slight anhydrous modification of the illite structure, (Brown, 1961). In addition, an occasional small variation in the shape of the illite reflection upon glycolation indicated the presence of a small expandable component present within the illite structure. The identity of this interlayer associate may be smectite since scanning at low 2θ values occasionally revealed the presence of a very small $14.5\overset{\circ}{\text{Å}}$ ($6.1^{\circ}2\theta$) diffraction peak.

Precise differentiation of the illite polymorphs was a difficult matter. Grim (1968) points out that the position of the 060 illite reflection can be used to distinguish between dioctahedral and trioctahedral polymorphs. However, differentiation of the polymorphs was inhibited due to confusion with the quartz 211 diffraction peak which occurs in the area of the 060 illite reflections.

Petrographic Thin Section and Scanning Electron Microscope:Differentiation of Clay Minerals:

Examination of the optical properties, morphological features and textural relationships of the clay sized fraction within epoxy impregnated thin sections assisted in the identification and differentiation of the clay minerals. Both authigenic and detrital components of kaolinite and illite were observed in thin section. However, the scanning electron microscope provides perhaps the best means by which authigenic and detrital clay minerals may be differentiated (and identified). Authigenic clay minerals commonly exhibit delicate morphologies and unique textural relationships that would not be present if they had not been formed "in situ". Scanning electron photomicrographs taken from gold coated Basal Quartz sandstone samples confirmed the existence of both authigenic and detrital illite and authigenic and detrital kaolinite.

Sample Preparation: According to Carrigy and Mellon (1964) special care must be taken in order to preserve authigenic clays during thin section preparation. For this reason all thin sections were prepared from sandstones impregnated with blue coloured epoxy. Thin section samples were obtained not farther than 5 cm distance from those samples used in scanning electron microscopy.

Six sandstone samples, for use in scanning electron microscopy, were carefully broken so as to obtain small portions exposing freshly fractured surfaces. Samples were then fastened to copper stubs and sputter coated with a 90 angstrom thick layer of gold using the Polaron E 5100 sputter coater. These samples were examined using a Philips 501B scanning electron microscope.

Detrital Illite: In thin section detrital illite can be recognized by its very fine grain size, brownish colouring and high birefringence. Detrital illite matrix, present before the compaction of the quartz grains, was in most cases situated between detrital grain contacts, (Photo 3.5). In several instances quartz grains were observed "to float" within a concentrated zone (up to several millimetres across) of detrital illitic clay. Clay within these zones was concentrated by the activity of sediment-burrowing organisms, (Photo 3.6). Quartz overgrowths were generally absent from portions of sediment with abundant detrital clay.

Detrital Kaolinite: Detrital kaolinite was identified in thin section by its lack of colour, low birefringence and refractive indices greater than 1.54, (Kerr, 1977). Detrital kaolinite was more difficult to detect and identify than was authigenic kaolinite which was more coarser grained relative to the detrital kaolinite. In scanning electron microscopy detrital clay minerals were less than 5 microns in size,

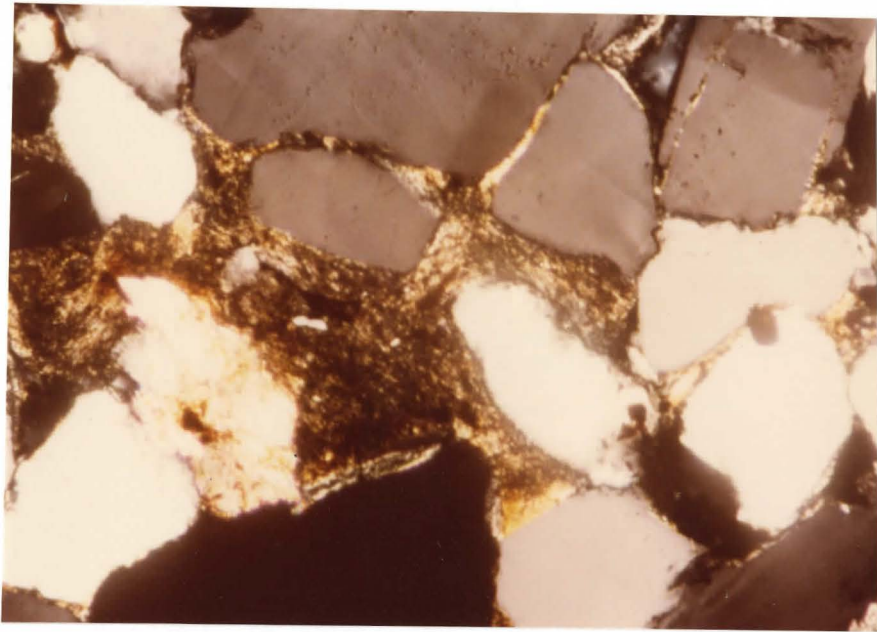


PHOTO 3.5 Detrital illite clay matrix situated between detrital quartz grain contacts. Sample 4-30-7, crossed polars, 160X magnification.

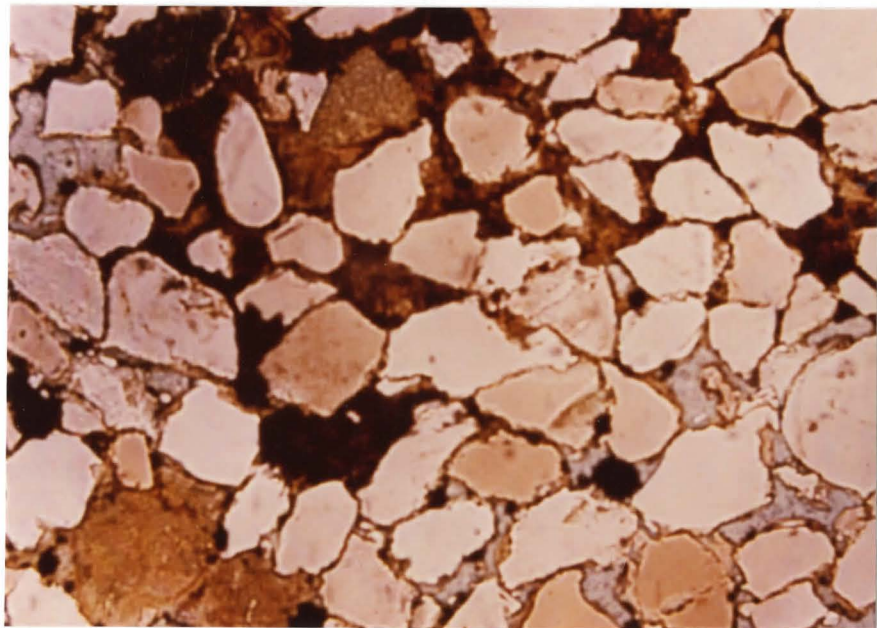


PHOTO 3.6 Quartz grains "floating" within illitic clay matrix that was concentrated by activity of burrowing organisms. Sample 4-30-7, 63X magnification.

and were difficult to identify due to the absence of well developed crystallinity.

Authigenic Illite: Thin section observation showed that, in many instances, sandstones with intergranular pores free of detrital clay contained quartz grains with authigenic quartz overgrowths. These overgrowths were in many cases covered by authigenic (pore lining) illite clay. Authigenic kaolinite would in some cases fill the remaining intergranular porosity (ie., pore filling cement). In thin sections, authigenic illite clay was not found situated between detrital grain contacts as was the detrital illite matrix, (Photo 3.7). Pore lining authigenic illite, developing primarily on quartz grains and quartz overgrowths, was also observed covering detrital chert, (Photo 3.8).

Scanning electron microscopy reveals that the pore lining authigenic illites possess the most delicate growth morphology of all the authigenic clay minerals, (Wilson and Pittman, 1977). Irregular flakes of illite, attached perpendicularly to pore walls, commonly develop wispy lath-like projections that grow out into the pore space, many attaining lengths of up to 30 microns, (Güven et al, 1980). Some of these lath-like projections can bridge the pore-gap (throat) between two adjacent quartz grains. However, the authigenic illite fraction within the Niton Basal Quartz sandstones commonly possessed short digitate lath-like extensions, (Photos 3.9, 3.10, 3.11, 3.12). In some instances the entire pore rimming

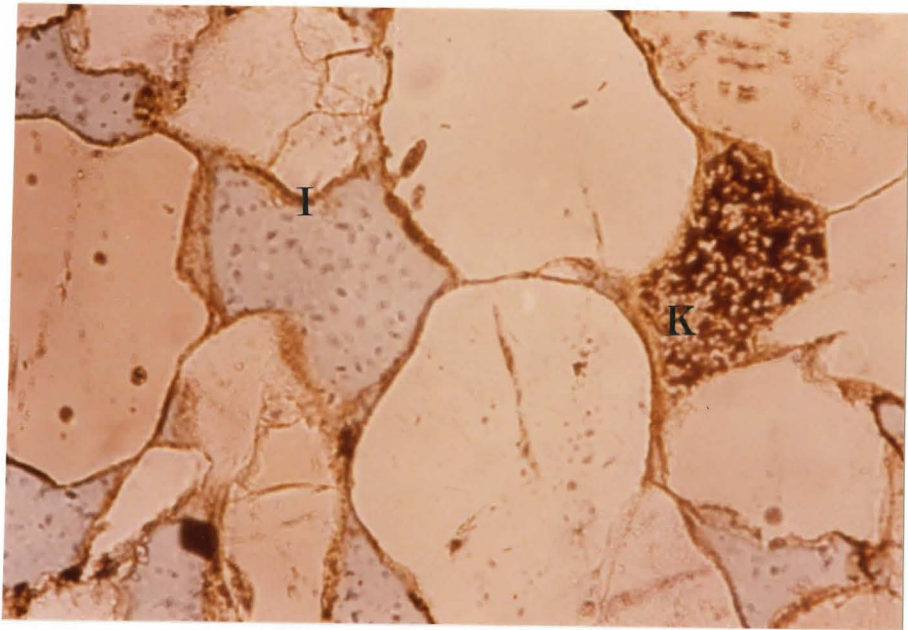


PHOTO 3.7 Pore lining authigenic illite (I) and pore filling authigenic kaolinite (K). Note absence of authigenic clay between detrital grain contacts. Sample 2-18-6, 160X magnification.

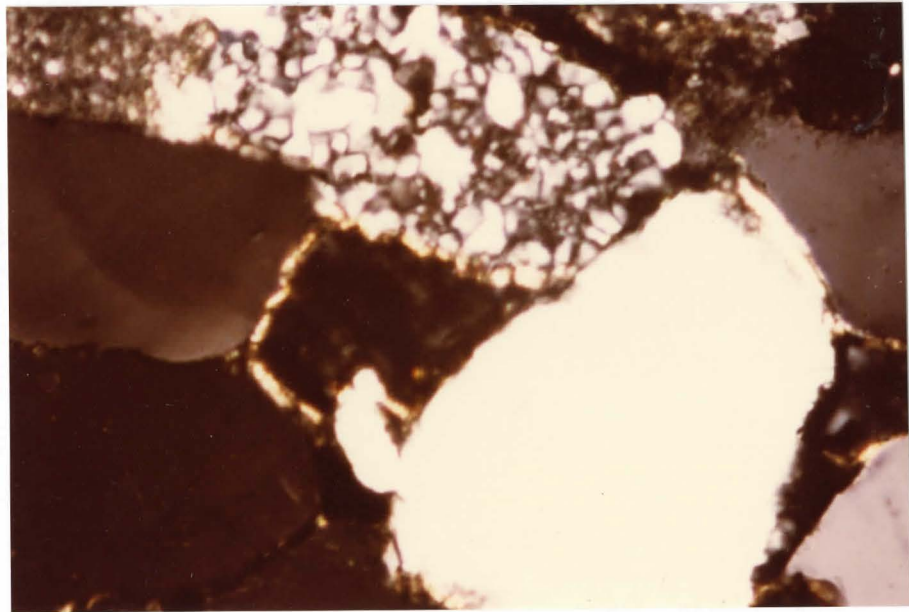


PHOTO 3.8 Birefringent pore lining authigenic illite, viewed under crossed polars, is seen partially rimming a detrital chert grain. Sample 2-18-6, 250X magnification.

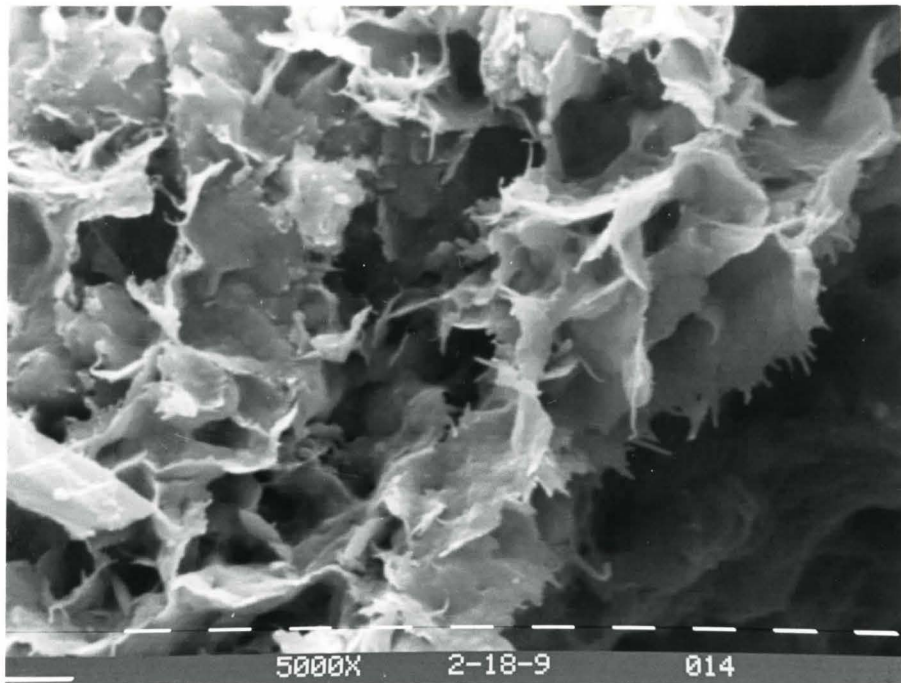


PHOTO 3.9 Short digitate lath-like extensions of authigenic illite. Scale bar equals 1 micron.

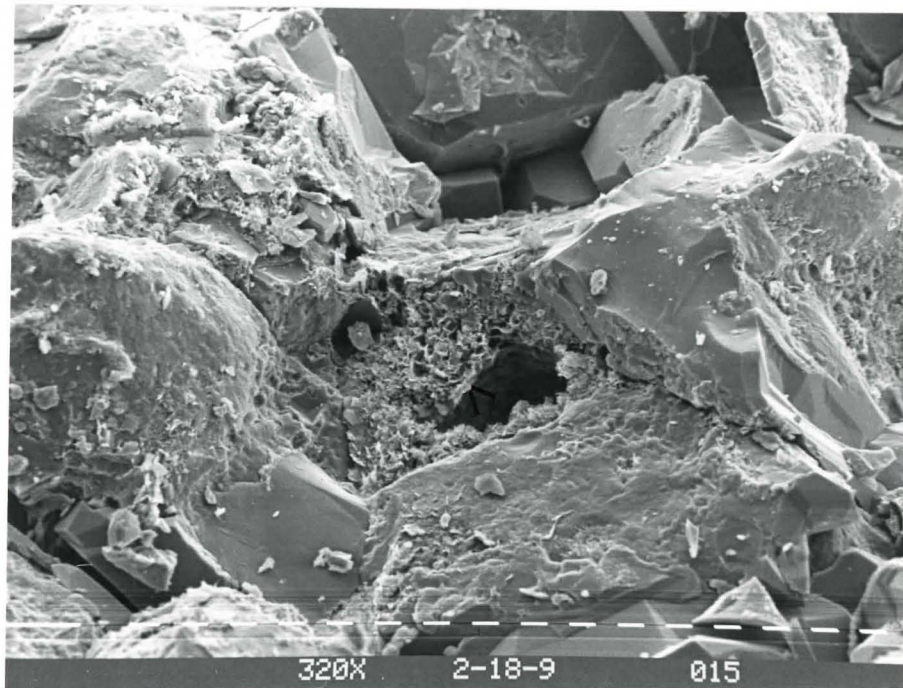


PHOTO 3.10 Arrow shows location of previous photograph. Scale bar equals 10 microns.

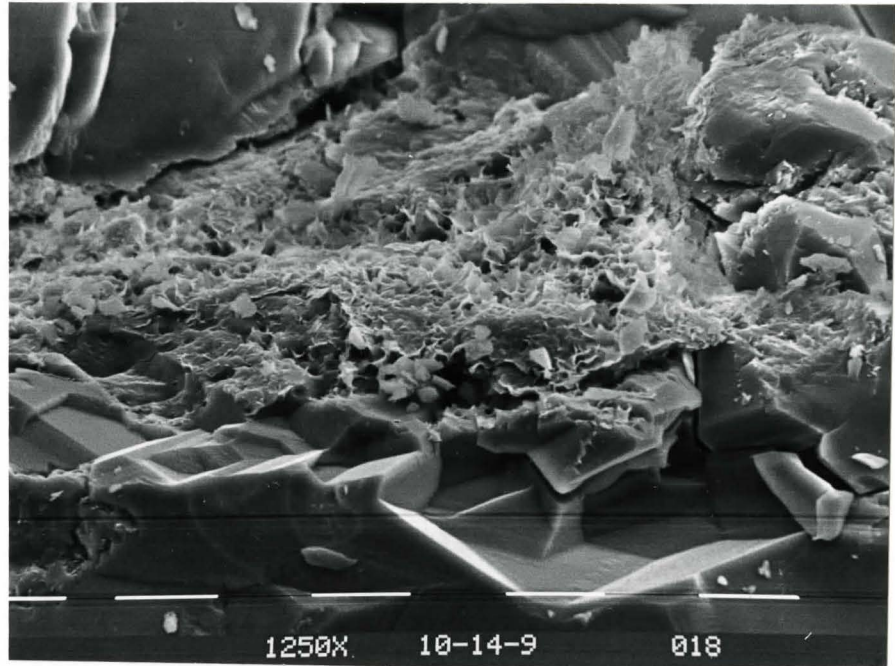


PHOTO 3.11 Authigenic quartz overgrowth covered by authigenic, pore rimming illite. Scale bar equals 10 microns.

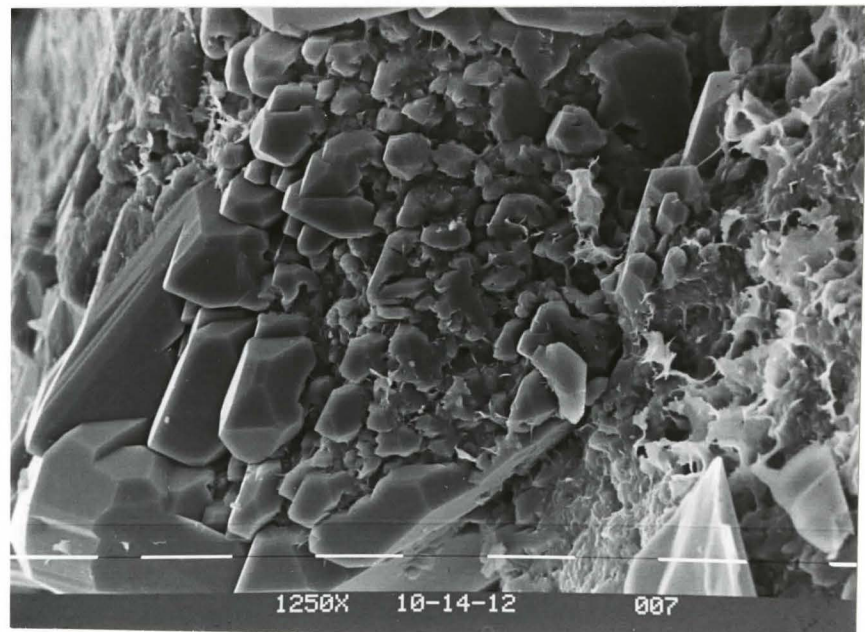


PHOTO 3.12 Authigenic quartz overgrowth just beginning to be covered by authigenic illite. Scale bar equals 10 microns.

authigenic illite structure would bridge the throat between two adjacent quartz grains, Photo 3.12, 3.14). The absence of long lath-like terminations may result, as X-ray diffraction data suggests, from a mixed layer assemblage of illite/smectite, with illite comprising the larger fraction.

In thin section authigenic clay cements were not observed to be situated between detrital grains. However, scanning electron microscopy (Photos 3.15, 3.16) shows the presence of possible authigenic illite that prior to sample preparation (ie. obtaining fracture surface of sandstone) was located between two detrital grains. This apparent anomaly is resolved in Chapter 5.

Authigenic Kaolinite: In thin section authigenic kaolinite may often be confused with chert, but it can be optically differentiated from chert on the basis of its higher refractive index and lower interference colours. Authigenic kaolinite occurred morphologically as fragile aggregates resembling "stacked booklets" arranged in random orientation, (Photos 3.17, 3.18), (Wilson and Pittman, 1977). Authigenic kaolinite was generally more coarser grained than authigenic illite.

The textural relationships of pore filling authigenic kaolinite with pore lining authigenic illite and authigenic quartz overgrowths are shown in Photos 3.19 and 3.20. Micropores within the authigenic kaolinite cement were

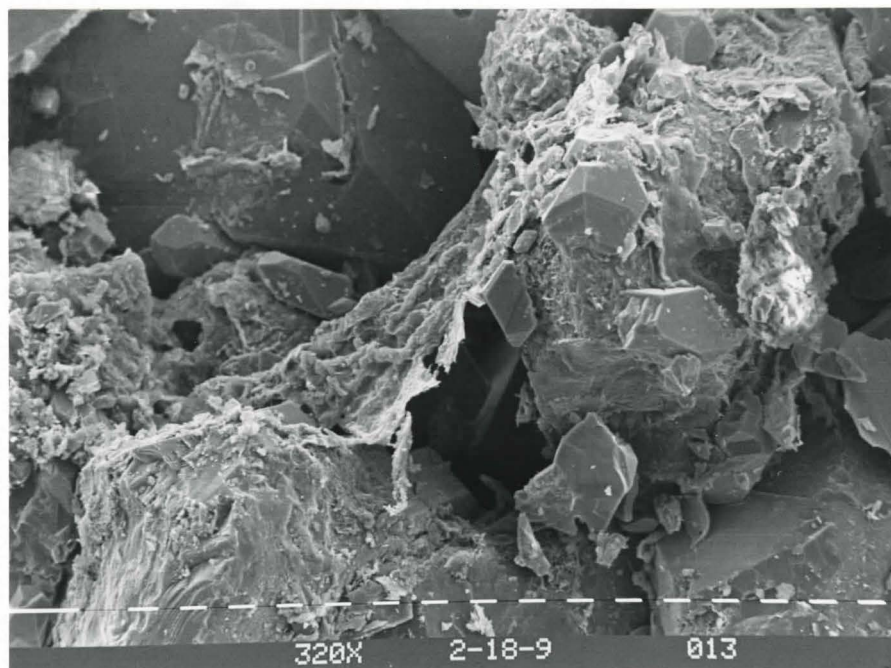


PHOTO 3.13 Authigenic illite bridging pore throat between two quartz grains. Scale bar equals 10 microns.

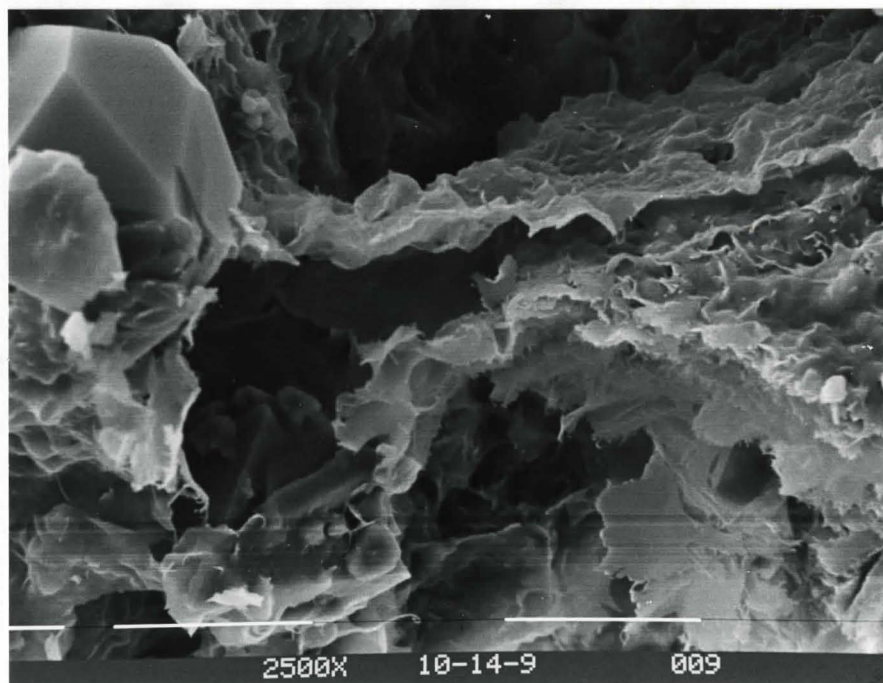


PHOTO 3.14 Close-up view of pore-bridging authigenic illite from another sample. Scale bar equals 10 microns.

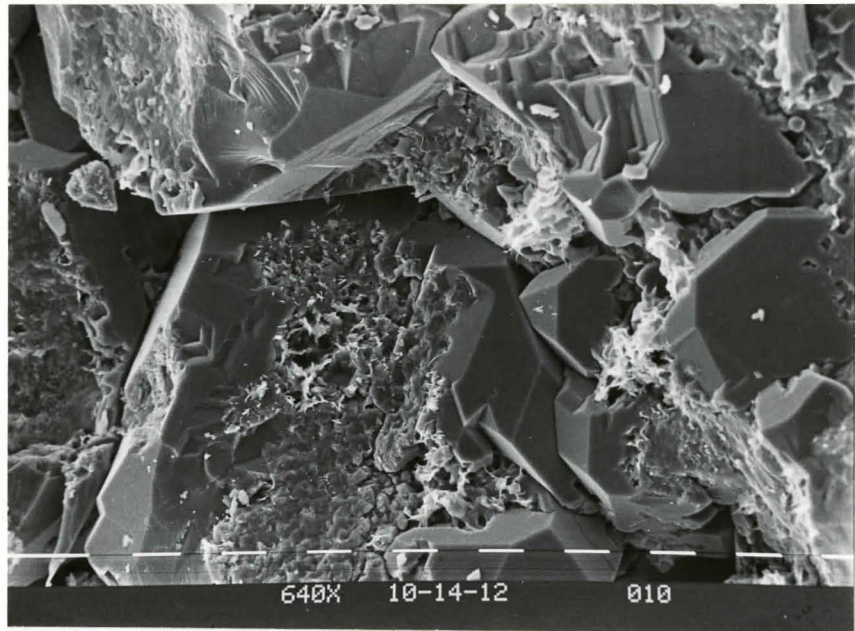


PHOTO 3.15 Tentatively identified authigenic illite that prior to sample preparation was located between detrital grains. Scale bar equals 10 microns.

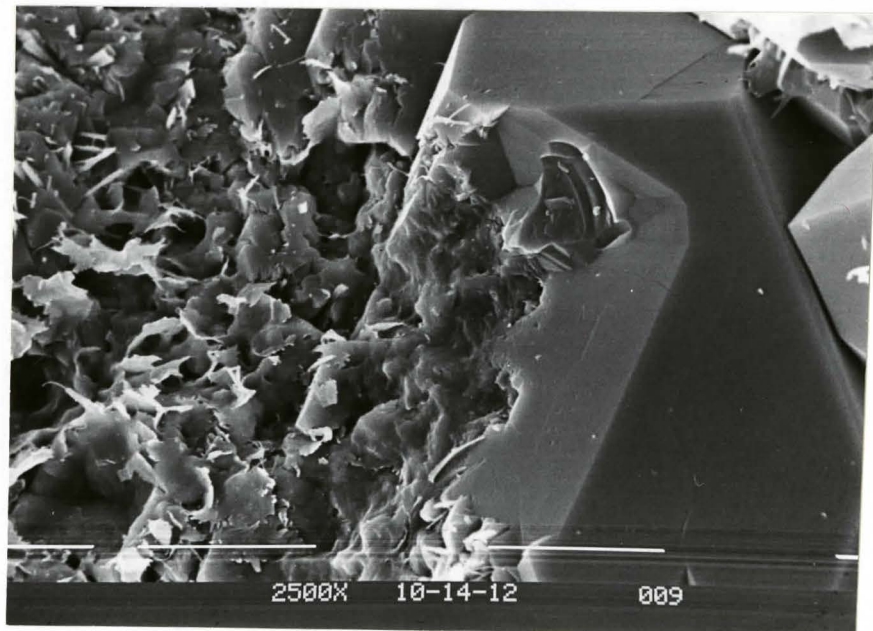


PHOTO 3.16 Similar photo to the one above. Scale bar equals 10 microns.

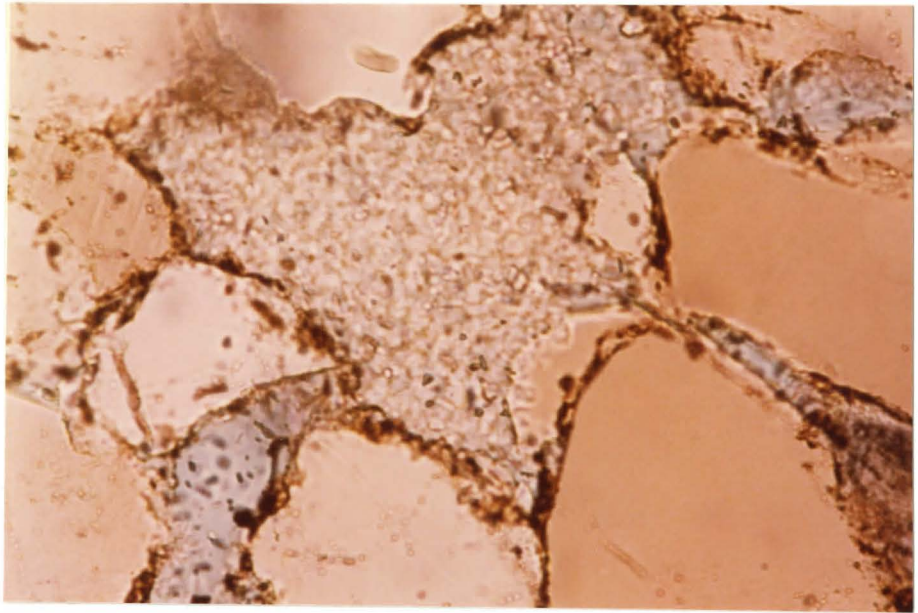


PHOTO 3.17 Colourless, randomly oriented "stacked booklets" of pore filling authigenic kaolinite. Sample 4-30-4, 250X magnification.



PHOTO 3.18 Same view as above except with crossed polars.

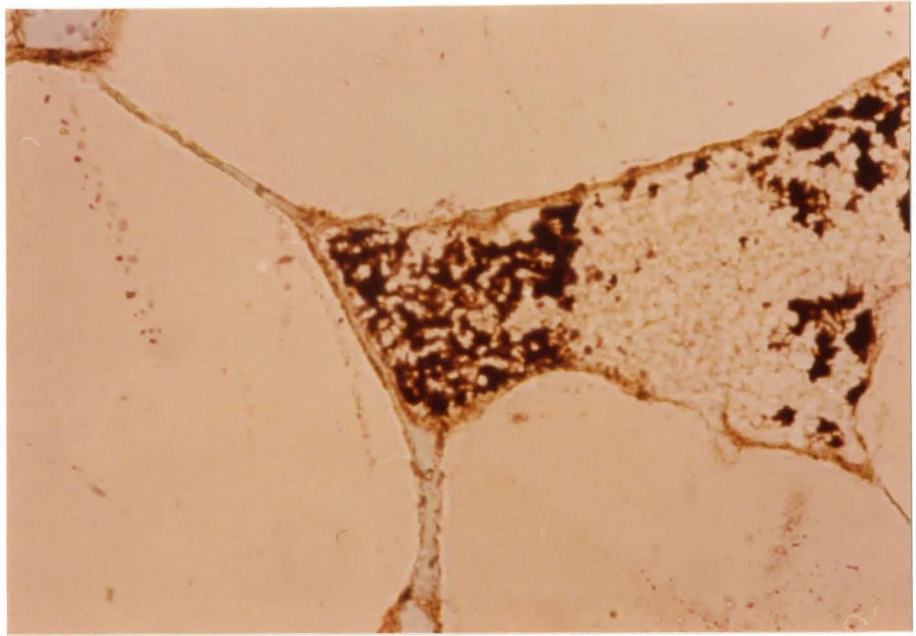


PHOTO 3.19 Initial intergranular pore space being obstructed by authigenic quartz overgrowths, pore lining and pore bridging authigenic illite and pore filling authigenic kaolinite. Sample 2-18-6, 400X magnf.

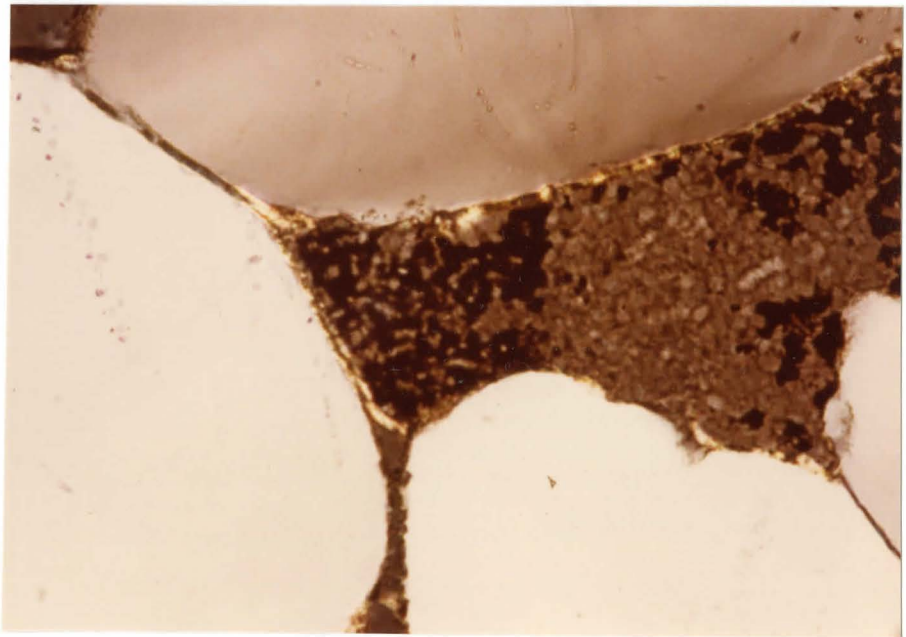


PHOTO 3.20 Same view as above except with crossed polars.

sometimes filled with a dark brown, near isotropic, material.

Under the scanning electron microscope authigenic kaolinite occurred as crystalline, pseudo-hexagonal plates (2-10 microns across), arranged in a face-to-face stacking pattern giving them the characteristic "stacked booklet" appearance, (Photo 3.21). Occasionally kaolinite booklets may attain long dimensions of up to 2500 microns (parallel with their C-axis) in which case they resemble "vermicular worms", (Wilson and Pittman, 1977). Within the Niton Basal Quartz sandstones this structure was not as evident as the "stacked booklet" structures.

The textural relationships observed in thin section of authigenic kaolinite to authigenic illite and quartz overgrowth were confirmed by scanning electron microscopy, (Photos 3.22, 3.23).

SemiQuantitative Analysis:

Semi-quantitative analysis was performed in order to determine if there existed any significant vertical and/or lateral, (well to well), variations in the relative proportions of the kaolinite/illite clay fraction.

X-Ray Diffraction Results: The method employed was based on the principle that the abundance of a clay mineral species is proportional to the intensity (or height) of the X-ray diffraction peak of that clay mineral, (Vemuri, 1967;

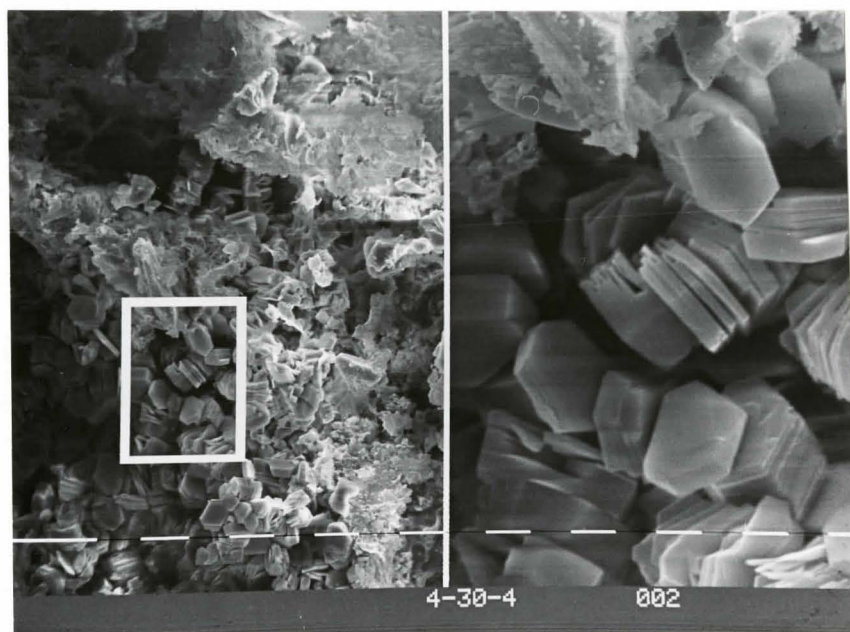


PHOTO 3.21 Stacked booklet morphology of authigenic kaolinite. Scale bar at left side of photo equals 10 microns.

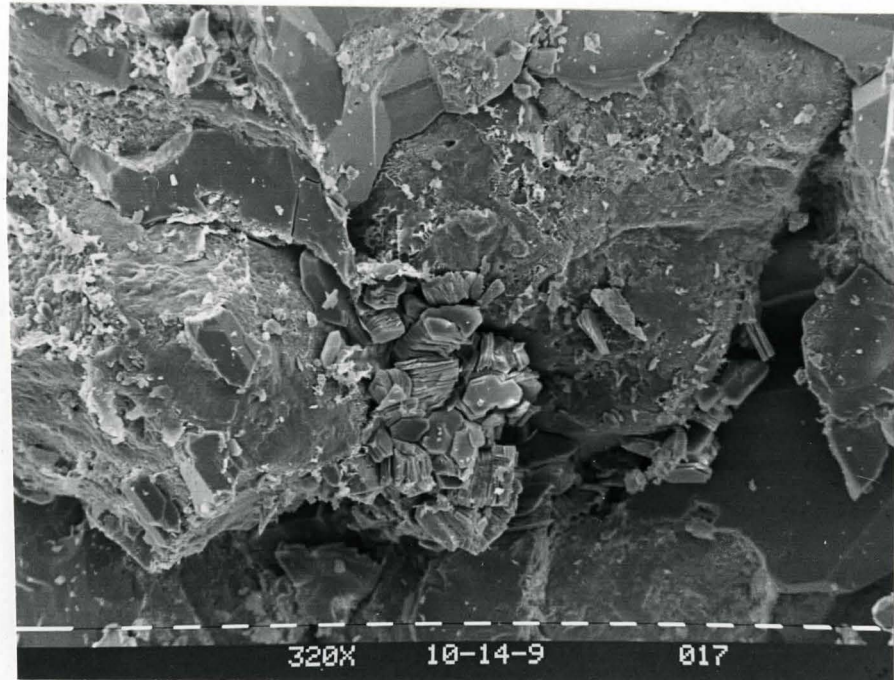


PHOTO 3.22 Two detrital quartz grains partially covered by authigenic quartz overgrowth, pore filling authigenic kaolinite also visible. Scale bar equals 10 microns.

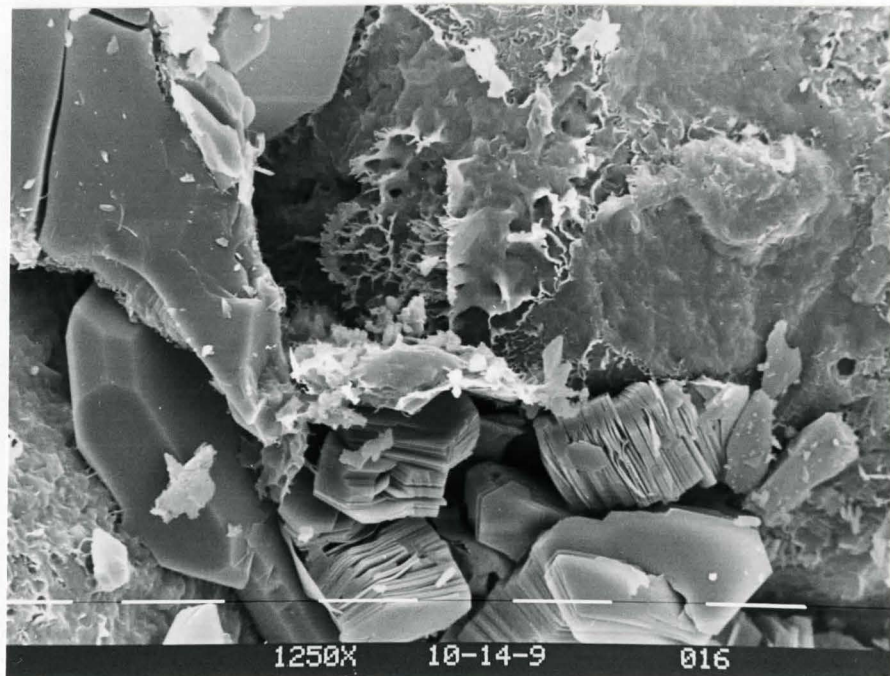


PHOTO 3.23 Close-up of above photo showing development of minor amounts of pore lining authigenic illite.

Unpublished Technical Memo). Vemuri (1967) found that even when clay minerals of varying degrees of crystallinity were dealt with, as illite in this study, that the peak - height method provided better results than the alternative method of peak - area measurement. Nonetheless, the accuracy of the peak - height technique was found to be poor.

The ratios of the 001 kaolinite/001 illite, ($7\text{\AA}/10\text{\AA}$), diffraction peaks were obtained from the 17 untreated clay mounts and converted into percentiles. These results, graphically displayed in Figures 2.1, 2.2, 2.3 are also expressed in Appendix I. Results show that no significant lateral variations exist between the clay fraction in the three different wells. However, results showed that the upper "A" zone sandstone (facies S.S.) consistently contained more kaolinite relative to the sandstone zones stratigraphically beneath. The "A" zone sandstones contained upwards of 80% kaolinite in the total clay fraction. In all but 3 of the 17 samples kaolinite was found to be in abundances greater than 50% of the total clay fraction.

Thin Section Visual Estimates: Precise identification, and hence quantitative evaluation of clay types, was difficult using the petrographic microscope. Nevertheless, based on visual estimates it was concluded that the bulk of the 'total' clay fraction was detrital clay (predominately detrital illite), whereas authigenic clays (mostly authigenic kaolinite) were locally present in lesser amounts.

CHAPTER 4PETROGRAPHIC INTERPRETATIONSMineralogic Maturity:

After detailed analysis of petrographic thin sections the author has concluded from the following characteristics that the Niton Basal Quartz sandstones are mineralogically mature.

- i) The quartz rich nature of the sandstones (average of point counts shows 77% quartz composition);
- ii) The presence of only 1 percent polycrystalline quartz grains;
- iii) The relatively high proportions (approximately 40%) of non-undulose quartz grains (relative to immature sandstones);
- iv) The dominance of the heavy mineral suite by well rounded, stable zircon, rutile, tourmaline and garnet;
- v) The absence of unstable detrital grains (e.g. Rock fragments, micas).

(Blatt et al, 1980; Pettijohn et al, 1972).

Textural Maturity:

Textural maturity is achieved in progressive stages. According to Folk (1968 in Pettijohn et al, 1972) these

stages are:

- i) removal of clay;
- ii) improvement of sorting;
- iii) rounding of grains.

If the clay content is greater than 5 percent (excluding authigenic clays) the sand is considered to be immature. Comparison of the Basal Quartz petrographic thin sections with Folks visual comparison chart has shown these subangular to subrounded sands to be generally "well sorted", thereby being classified as mature. Nevertheless, point count data (Table 3.1) has shown that many of these sandstones contain large (>5%) abundances of clay. This textural inversion (high clay abundance in a well sorted sandstone) can be attributed to diagenetically introduced clays (authigenic clays), and to additional detrital clays introduced by bioturbation or by insufficient winnowing in the depositional environment, (e.g. low energy abandoned channel fill). Consequently the Niton Basal Quartz sandstones are both mineralogically and texturally mature. This conclusion is in agreement with the results of Williams (1963).

Provenance:

It will be shown further in this chapter that the Basal Quartz sandstones have not been subjected to burial depths

where large scale mineralogic transformations can occur within the detrital clay fraction. For this reason it was concluded that the detrital clay minerals of these sediments represent the clay minerals present at the time of deposition. (The origin of the authigenic clay minerals will be dealt with in Chapter 5).

Detrital Illite: Detrital illites are a common matrix constituent within the Niton Basal Quartz sandstones, and have been inherited from various source areas. Illite is the general term proposed for the micaceous clay minerals; muscovite, biotite, illite and glauconite, (Grim, 1968).

Detrital muscovite, visible in thin sections as deformed, birefringent laths may have been derived directly from the weathering Cordilleran highlands to the west. Rounded, distorted grains of detrital glauconite probably formed as an alteration product of fecal pellets present within the depositional environment, rather than by the alteration of detrital phyllo-silicates. A small portion of the detrital illite fraction may have been inherited as a well crystallized polytype, however, the larger detrital illite fraction arrived as a cation deficient, degraded (1 Md polytype) illite, as the weak, broad X-ray diffraction peaks imply. The degradation of the illite structure probably occurred as K^+ undersaturated solutions leached K^+ ions from the illite structure. These K^+ ions were probably replaced by water molecules as suggested by the

anhydrous modification of the illite structure during heating, (Millot, 1970).

Detrital Kaolinite: Detrital kaolinites are inherited from various source areas. These may include actively eroding exposures of continental bedrock, weathering mantles or soil horizons (Millot, 1970). In many cases detrital kaolinitic clay minerals are derived from warm, moist, tropical areas where vigorous leaching removes and transports cations away from the weathering horizon, (Keller, 1970).

A certain portion of the detrital kaolinite of the Basal Quartz sandstones has probably been derived from the intense weathering of an unstable cratonic western source. However, the textural and compositional maturity of the Basal Quartz sandstones suggests that these sandstones may have been derived from a pre-existing sedimentary source. Hence the remainder of the detrital kaolinite clay fraction may be inherited from this previous sedimentary source, which in turn obtained its clay fraction penultimately from a weathering crystalline basement source.

Based upon the nature of the detrital mineralogy it was concluded that the Niton Basal Quartz sandstones have been derived in part from a pre-existing sedimentary (sandstone) source, and in addition, because of the presence of chert, mica and well rounded heavy minerals a metasedimentary source is also suggested. The pre-existing sandstone source had probably itself passed through several depositional cycles since its

origin from a pre-Cambrian source, (Williams, 1963).

During the period of lower Mannville deposition the paleoslope in the Niton area was approximately towards a north to northeasterly direction, (Nelson, 1970). The sediment source(s) were probably from a western to southern direction. The Cordilleran uplifts exposing metasedimentary rocks may have been one of the areas of provenance for the Niton area, (Glaister, 1959; Williams, 1963).

Porosity Reduction By Clay Minerals:

Detrital Clays: The results of semiquantitative analysis from X-ray diffraction data, that the total clay fraction is dominated by kaolinite, are in agreement with the results of Carrigy and Mellon, (1964). These conclusions suggest that visual estimates of the abundances of detrital kaolinite in thin section are too low, and that illite may not be the dominant member of the detrital fraction. Nevertheless, on the basis of visual estimates it was concluded that the bulk of the porosity reducing total clay fraction is of primary origin, that is detrital clay. Furthermore, additional porosity reducing authigenic clays, of secondary (diagenetic) origin, are locally present in lesser amounts.

It follows from this conclusion that the proportion of detrital clay should be decreased in abundance, and initial porosity increased, in those sand bodies deposited under depositional conditions of high energy, (e.g. distributary

mouth bar deposits). Semiquantitative analysis of X-ray diffraction data shows (Figures 2.1, 2.2, 2.3) that the sandstones of facies S.S., interpreted to be distributary mouth bar deposits (Chapter 2), contain significantly greater abundances of kaolinite relative to the other sandstone facies. Scanning electron microscopy and thin section studies reveal much of this kaolinite to be authigenic (ie., secondary origin). Clay free, permeable sands favour processes operative in the secondary (neoformative) development of authigenic kaolinite, (Chapter 5), (Füchtbauer, 1967; Millot, 1970). Therefore, the high proportions of authigenic kaolinite within the sandstone (S.S.) facies suggest that these sands were initially free of detrital clay relative to the other Basal Quartz sandstones. Consequently, the depositional energy effects that favour high initial porosity are offset by the porosity reducing effects of secondary (authigenic) clay mineral formation.

Authigenic Clays: Observations of the complex morphological and textural relationships of the Basal Quartz authigenic minerals by scanning electron microscopy and petrographic work have revealed that in many instances the porosity reducing authigenic mineral assemblage, proceeding from the detrital grain surface to pore centre is:

- i) authigenic quartz overgrowth;
- ii) authigenic pore lining illite;
- iii) authigenic pore filling kaolinite.

According to Wilson and Pittman (1977) authigenic clay cements in pore centers are younger than those adjacent to detrital grain surfaces. Hence, the authigenic mineral assemblage listed above is also a time progressive authigenic mineral assemblage, that is to say, quartz overgrowths have developed first, followed by pore lining illites which in turn were followed by pore filling kaolinites.

Prelude to Paragenesis:

In order to understand the present type and distribution of porosity within the Niton Basal Quartz sandstones one must derive a paragenesis explaining how the original porosity has been modified in space and time during the course of sandstone diagenesis. In addition to explaining this progressive assemblage of porosity (and permeability) reducing authigenic minerals the paragenesis must also account for the presence of diagenetically formed carbonate cement, pyrite, siderite and secondary porosity.

Several important factors to consider when examining the diagenetic history of a sandstone are:

- i) geothermal gradients,
- ii) burial depths,
- iii) original sand composition,
- iv) original pore fluid composition,
- v) time.

(Blatt et al., 1980)

Prior to determining a paragenesis for the Niton Basal Quartz sandstones one must first determine the increase in temperature experienced during sediment burial. To obtain this one must know the geothermal gradient and the maximum depth of burial of these sandstones.

Determination of Geothermal Gradient: The geothermal gradient for the Niton field was determined from borehole temperature measurements taken shortly after drilling of the wells was completed. The average bottom hole temperature for the three wells as recorded on borehole logging records was approximately 58°C (136°F) at an average depth of 2007 metres (6691 feet). However, bottom hole temperature measurements recorded immediately after drilling tend to be 10°C to 20°C lower than normal due to the interruption of pore water migration within the substratum, (Blatt et al., 1980). Consequently, assuming measured bottom hole temperatures to be 20°C lower than normal (ie., true bottom hole temperature is 78°C) and assuming the surface temperature at 0 metres to be 10°C an average geothermal gradient of 3.4°C/100 m was obtained. This value is slightly higher than the 3.1°C/100 m to 3.3°C/100 m geothermal gradients calculated by Magara (1978) for the Western Canada Basin.

Determination of Maximum Burial Depth: Assuming that no erosion has occurred since the deposition of the Niton Basal Quartz sediments, their present average burial depth of approximately

1977 metres (6590 feet) would be the maximum depth of burial that they have experienced. However, this assumption is invalid since the Western Canada Basin has been uplifted and eroded late in its geologic history. Consequently, in order to determine the maximum depth of burial an estimate of the erosion that has occurred was made on the basis of shale compaction data.

Magara (1978) has stated that the level of shale compaction is controlled primarily by burial depth. If in the area under study there has been significant erosion, a noticeable shift in the shale compaction trend should be evident, (ie., increased compaction values at any present depth). Values of increased shale compaction, (decreased shale porosity), can be obtained by measuring interval transit times from sonic logs. Interval transit times are directly proportional to shale porosity values. If no erosion had occurred within the Niton area a plot of shale transit time versus depth would have given a shale compaction trend which, when extrapolated to the present surface, (0 metres) would have given a transit time of 200 microseconds per foot, (Magara, 1978).

Transit times from shale beds within the three study wells, plotted versus depth on Figure 4.1 reveal that an average of approximately 2500 feet (750 m) of erosion has occurred. This is consistent with estimates given by Magara, (1978). Examination of Magara's (1978, Figure 2.33) geological sections of Western Canada show approximately 1000

PLOT OF SHALE TRANSIT TIME VERSUS
DEPTH OF BURIAL

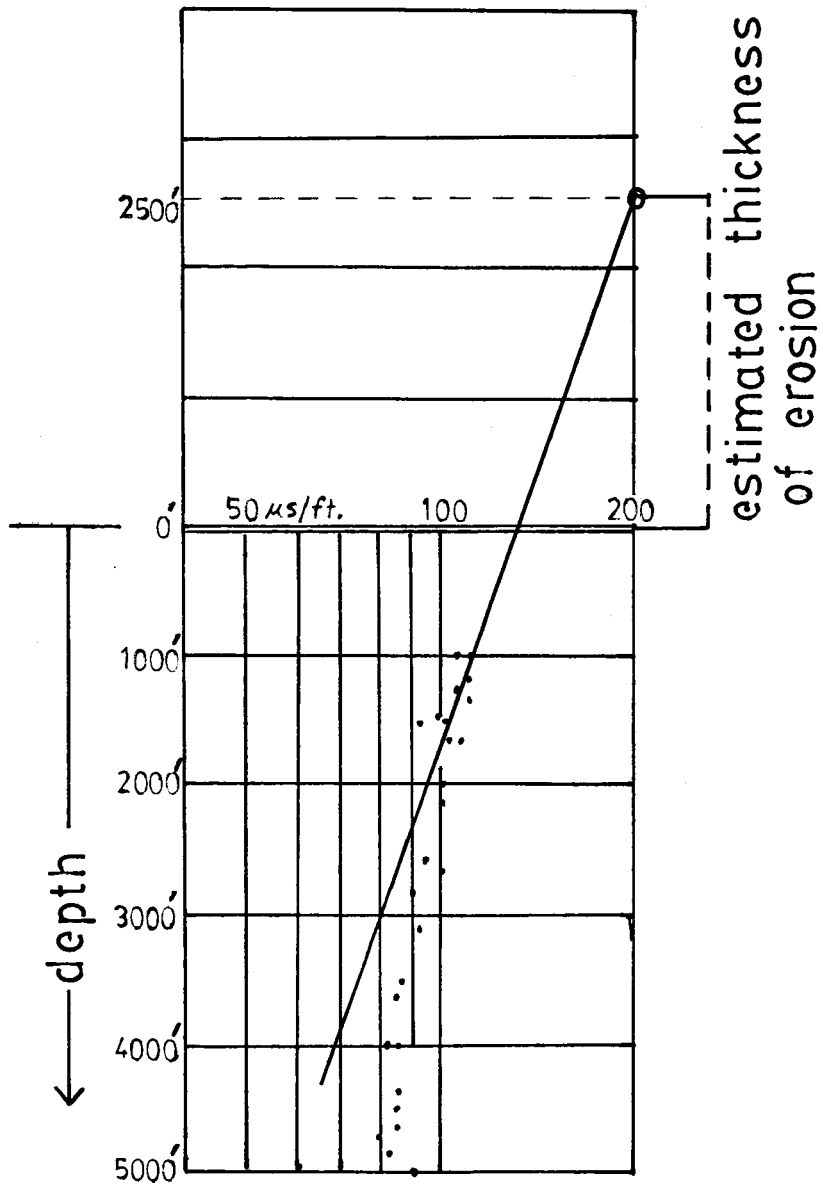


FIGURE 4.1

to 3000 feet (330 m to 990 m) of erosion has occurred in an area about 180 kilometres south-east of the Niton Field. Assuming that the erosional surface is located at the present surface, the average maximum depth of burial of the Niton Basal Quartz sandstones can be calculated by summing the present maximum depth of burial (1977 m, 6590') and the estimated thickness of erosion (750 m, 2500'). Consequently the (average) maximum burial depth of the Niton Basal Quartz sandstones was approximately 2727 metres (9090 feet).

Assuming that the calculated geothermal gradient of approximately $3^{\circ}\text{C}/100\text{ m}$ has not varied much in the geologic past, (Magara, 1978), the maximum temperature that the Niton Basal Quartz sands have experienced during diagenesis was approximately 100°C .

CHAPTER 5DIAGENESISIntroduction:

Diagenesis of the Niton Basal Quartz sediments begins at the moment they are deposited on the shallow sea floor. During the early stages of diagenesis at, or near, the sediment water interface the chemistry of the pore fluids is controlled primarily by the nature of depositional environment. Schmidt and McDonald (1979) adopt the term "Eodiagenesis" for this early stage of diagenesis where compaction of the sediments has not yet sealed the interstitial pore fluids from the effects of surface chemical reagents.

Eodiagenesis:

Mechanical Reduction of Porosity: Eodiagenesis is characterized primarily by mechanical reduction of porosity. Prior to the compaction of the sediment the initial sandstone porosity is approximately 40 percent. As the depth of burial increases, mechanical compaction decreases initial porosity until chemical porosity reduction becomes dominant. (Chemical porosity reduction is dominant in the "Mesodiagenetic" regime.) Using approximate visual estimates the minus-cement-porosity of the Basal Quartz sandstones is about 20-25 percent, (ie., the sum of current porosity and volume of authigenic cement),

(Füchtbauer, 1967). This value indicates that mechanical compaction reduced the initial porosity by roughly 15-20 percent before the precipitation of authigenic cements became dominant in porosity reduction.

Pore Fluid Chemistry: Initial pore fluids, derived from the shallow marine (deltaic) environment, are primarily marine to brackish in nature. However, shortly after deposition of the Basal Quartz sandstones, (and prior to compaction), periods of emergence allowed fresh water to replace the marine to brackish interstitial fluids within the sand sediments, (G.V. Middleton, Personal Communication). Nevertheless, as compaction increased, the marine to brackish fluids expelled from adjacent shale beds drove out the fresh water from the sand sediments.

During eodiagenesis, free oxygen present within the pore fluids is removed by the activity of aerobic bacteria upon the organic detritus common in the buried Basal Quartz sediments. Carbon dioxide is liberated by the oxidation of these organic constituents. As the PCO_2 rises, hydrogen ions are produced and the initial pH of the pore fluid decreases from approximately 8 to about 7 or 6.5, (Collins, 1975; Fairbridge, 1967). The Eh of the water also decreases below its initial value of roughly 400 millivolts, but still remains positive, (Collins, 1975).

The low pH environment is hostile to detrital $CaCO_3$. If substantial $CaCO_3$ is present within the sediments it will buffer the pH of the pore fluids consequently the interstitial

fluid pH will not decrease below 7. The low pH zone, if present, extends downwards from the sediment water interface to depths of approximately 0.3 to 0.5 metres, (Fairbridge, 1967). Aerobic bacteria gradually die out as the free oxygen of the pore fluid is consumed. The oxidizing nature of the upper zone transforms into a reducing zone dominated by anaerobic bacteria. Pore fluid pH values now increase to approximately 9, and Eh values decrease to about -400 mV to -600 mV, (Collins, 1975; Fairbridge, 1967). Remaining CaCO_3 is protected from further dissolution in these alkaline reducing conditions, and in addition, precipitation of small amounts of CaCO_3 cement probably occurs at this stage. Organic matter preserved within the reducing zone sediments now have a much greater chance to be further modified into hydrocarbons, (Fairbridge, 1967). However, organics may be replaced by pyrite in certain instances, (Ho and Coleman, 1969).

Pyrite Formation: Anaerobic bacteria, feeding upon organic matter, attack the sulphate ion reducing it to sulphite and then sulphide, (Collins, 1975). Consequently in an alkaline, reducing, organic rich environment, (e.g. poorly drained swamp), one might expect authigenic pyrite to form, (Berner, 1971). Authigenic pyrite is indeed present within the sands and shales of the Niton Basal Quartz sediments. Pyrite concentrations were generally higher in areas of greater organic accumulation. Reservoir quality has not been

significantly reduced by the presence of limited amounts of pyrite.

Siderite Formation: Siderite present within the Niton Lower Mannville sediments has also formed during eodiagenesis. Authigenic siderite will form only in brackish to non-marine, anaerobic groundwater characterized by low Eh values (about -330 mV to -430 mV), high PS^{2-} values ($PS^{2-} > 14$), and ferrous iron concentrations greater than 5 percent that of calcium, (Berner, 1971; Fairbridge, 1967). Organic matter also plays an important role in the (solubility) formation of siderite, (Ho and Coleman, 1969). Poorly drained swamp environments, suitable for the diagenetic formation of siderite, would be present within the proposed (Niton) deltaic environment.

Mesodiagenesis:

As compaction proceeds to the point where interstitial fluids are sealed from surface reagents, the regime of mesodiagenesis has been entered, (Schmidt and McDonald, 1979). It is during mesodiagenesis that the greatest modifications in porosity and permeability occur within the Basal Quartz sandstones. Authigenic quartz overgrowths are recognized as the earliest developing mineral that substantially reduces porosity

Authigenic Quartz Overgrowths: During mesodiagenesis the activity of orthosilicic acid (H_4SiO_4), within the pore fluids was greater than its solubility product. Therefore the solution was over-

saturated with respect to silica, (SiO_2), thus causing silica to precipitate out of solution, (Collins, 1975). The occurrence of silica overgrowths without evidence of pressure solution of detrital quartz grains implies that other sources of silica are important, (Berner, 1971)

Silica may in part be generated by the dissolution of detrital silicate minerals, however, this was not an important contributor of silica in the quartz rich Niton Basal Quartz sandstones, (Blatt et al., 1980). Much of the silica was probably derived from outside of the Basal Quartz sandstones, probably from pore waters migrating (diffusing) from adjacent shales.

According to the estimated minus-cement-porosity values (20-25%), porosity reduction by quartz cementation has become dominant only after 15 to 20 percent mechanical porosity reduction has occurred. This suggests that quartz cementation was at substantial depths of burial, possibly greater than 600 metres, (Füchtbauer, 1967).

Authigenic Illite: Authigenic illite, which has formed after authigenic quartz overgrowths, may form by three methods:

- i) In situ alteration of a parent mineral,
- ii) Recrystallization of pre-existing detrital illite clay minerals, (Transformation)
- iii) Direct precipitation from alkaline, cation rich pore fluids, (Neoformation).

(Millot, 1970; Güven et al., 1980).

Any interpretation as to the means of emplacement of authigenic illite must account for the seemingly conflicting morphological and textural features observed in the study of the clays.

These conflicting features are:

- i) The apparent lack of well developed crystallinity of a large portion of the total illite clay fraction. This is implied by the broad, diffuse nature of X-ray diffraction peaks and by the absence of wispy lath-like terminations in electron microscopy studies.
- ii) The presence of authigenic illite (well crystallized polytype) found as pore lining and pore bridging morphologies, (Wilson and Pittman, 1977).

The author has concluded that there exists three viable alternative hypothesis explaining the emplacement of authigenic illite. Choosing the correct interpretation is of grave importance in the critical evaluation of porosity and permeability reduction. These three hypothesis are summarized below.

- i) Most of the total illite fraction is of the degraded (detrital) polytype thus accounting for the general poor illite crystallinity. However, transformation by aggradation of the allogenic illite during diagenesis has begun to regularize the crystal lattice by addition of K^+ ions from alkaline, cation rich pore solutions, (Millot, 1970). Wispy lath-like crystal terminations

have consequently just begun to develop.

Unfortunately this theory does not account for the presence of observed neoformed textural relationships.

- ii) Direct precipitation of authigenic illite has produced the pore lining, pore bridging morphologies. However, the proportions of cations within the alkaline pore fluid has led to the development of a mixed layer illite/smectite clay system. This hypothesis resolves the apparent lack of crystallinity as observed in scanning electron microscopy and in X-ray diffraction patterns.
- iii) Certain amounts of neoformation of illite must have occurred in order to account for the bridging of pore throats and development of pore coatings. However, as diagenesis progressed and the alkaline, cation rich environment of illite neoformation altered to an acidic cation deficient environment favouring neoformation of kaolinite, the illite became vulnerable to K^+ leaching and began to degrade. This degradation would result in irregularities within the illite crystal lattice and wispy lath-like terminations once present have now begun to dissolve.

The author has concluded that in order to explain the delicate pore bridging, pore lining morphologies certain amounts of illite neoformation must have occurred, (Alternatives ii, iii).

To resolve the apparent anomaly of authigenic illite being found between detrital grain contacts, (Photos 3.15, 3.16), it is suggested that detrital illite may have been transformed by aggradation to an authigenic illite structure, (Alternative i).

Pore lining and pore bridging morphologies often restrict or block pore throats, thereby having a greater effect on permeability reduction than on porosity reduction, (Wilson and Pittman, 1977). The short digitate lath-like projections of the authigenic illites in these sands are more favourable than authigenic illites possessing long, wispy lath-like projections since permeability would be further decreased by the longer terminations. In addition, long illite laths are very fragile and break easily during reservoir stimulation. Migration of these fine particles often increases pore throat blockage, (Guvén et al., 1980). The short nature of the illite laths may be explained in part by both alternatives ii and iii, however, further conclusions may be possible after studying the formation of authigenic kaolinite.

Although alternatives ii and iii can rationalize the coexistence of seemingly well crystallized neofomed morphologies of authigenic illite with the conflicting, broad, diffuse nature of illite X-ray diffraction peaks, most of the poor crystallinity observed in X-ray analysis is probably due to the large abundance of detrital illite within the Basal Quartz sediments. Recall that the crushing technique employed in X-ray sample preparation could not avoid the mixing of authigenic and

detrital clays, (Chapter 3). This conclusion is in agreement with Millot (1970) who states that most of sedimentary illites are inherited, (detrital).

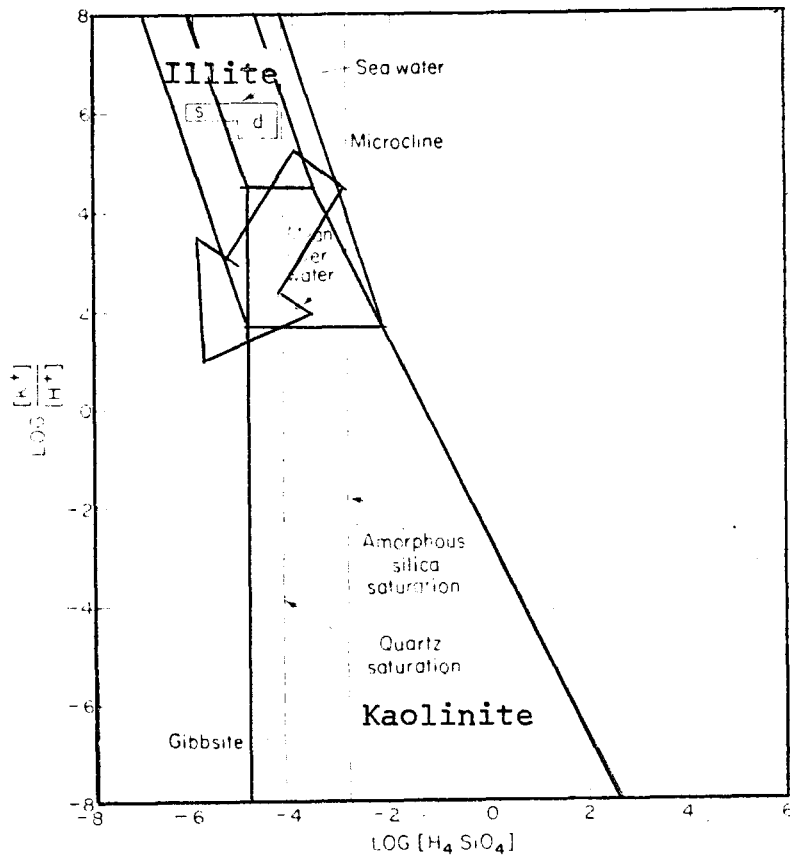
Authigenic Kaolinite: During progressive diagenesis of the buried sediments, the precipitation of authigenic quartz overgrowths and authigenic illite has gradually depleted the pore fluids in potassium ions and orthosilicic acid. The stability field diagram in Figure 5.1 shows that the next authigenic mineral to precipitate out of solution will be authigenic kaolinite, and indeed this has been confirmed in this study, (Chapter 3). Authigenic kaolinite may form by either or all of the processes of:

- i) "in situ" alterations of a parent mineral,
- ii) transformation of pre-existing kaolinite,
- iii) neoformation,

(Shelton, 1964).

Within the detrital grain framework of the Niton Basal Quartz sandstones, feldspar was recognized as a possible parent mineral capable of supplying suitable chemical components for the "in situ" development of kaolinite. The Basal Quartz sandstones contain occurrences of partly dissolved detrital feldspar with rare kaolinite replacement. Unfortunately, dissolution of the limited amount of detrital feldspar present could not account for the observed abundances of authigenic kaolinite.

FIGURE 5.1



(After Blatt et al., 1980)

The arrow shows the changing chemical composition of pore waters during mesodiagenesis. Stability field boundaries have been calculated at a temperature of 25°C. Although mesodiagenetic temperatures reach 100°C boundaries were not recalculated since they are relatively inaccurate and should be used as a guide only.

The relationship of high initial porosity to increased authigenic kaolinite abundance (Chapter 4) is a relationship that would not be observed had the authigenic kaolinite arose from transformation of limited quantities of pre-existing allogenic kaolinite. Hence secondary kaolinite must have developed by neoformation, and the dissolved reactants necessary for the neoformation must have been derived from sources outside of the sandstone body.

According to Millot (1970) and Keller (1970) neoformation of kaolinite must be from cation poor, alumina enriched, acidic pore waters, (pH about 6). Neoformation of kaolinite will cease where pore fluids fail to percolate since this results in the accumulation of cations in solution, (Millot, 1971). At this stage late in the diagenetic history of the Niton Basal Quartz sediments temperatures are approaching their calculated maximum of 100°C. The thermomaturation of organic matter, present primarily within the shales, liberates CO₂ which combines with interstitial waters to produce carbonic acid, (Decarboxylation process), (Schmidt and McDonald, 1979). As thermomaturation increases soluble petroleum and insoluble kerogen are generated from the organic precursors.

The presence of carbonic acid in the migrating (shale to sandstone), interstitial water results in the lowering of the pH. Therefore an acidic environment favouring the neoformation of kaolinite is produced. Dissolution of

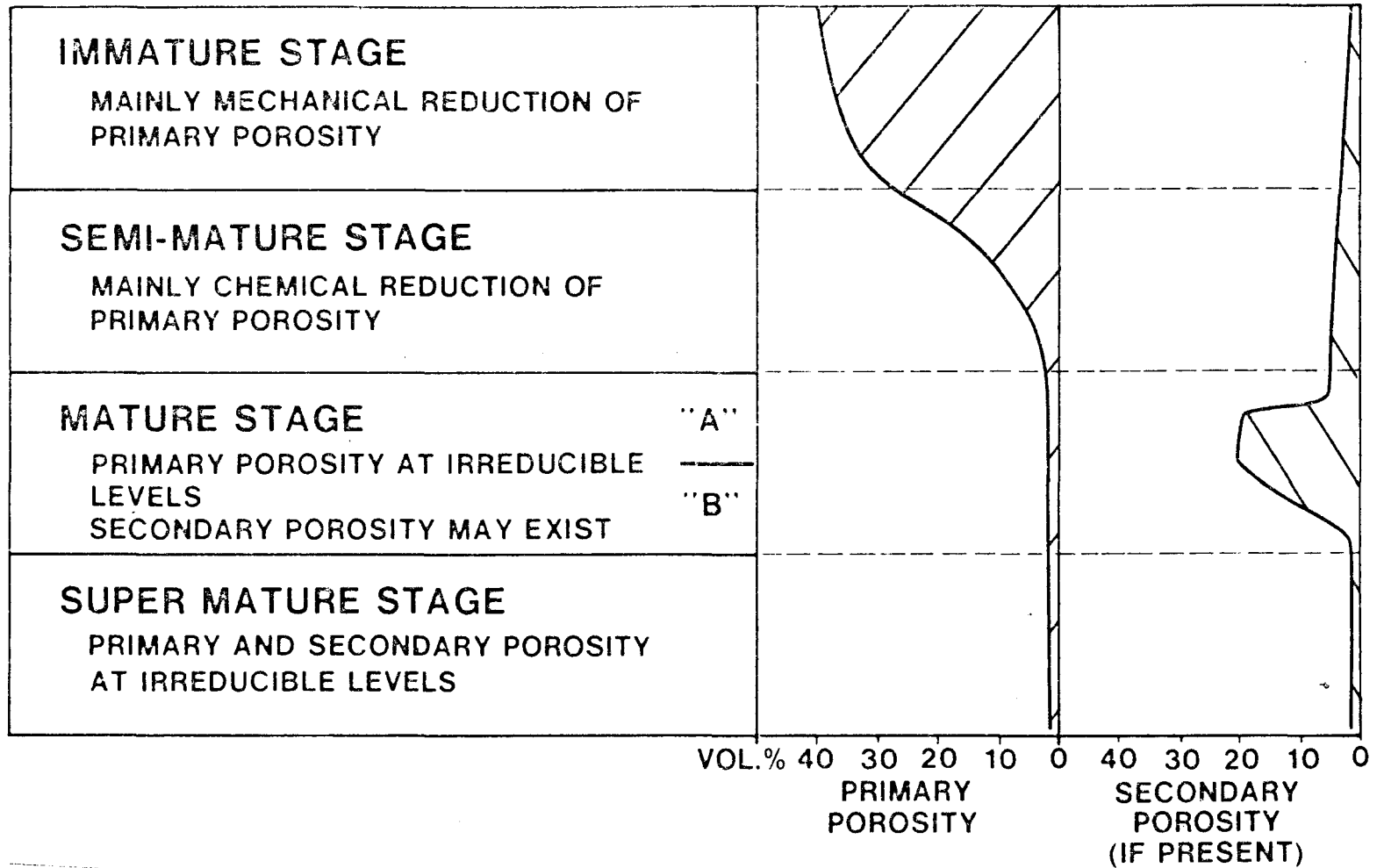
carbonate minerals (calcite) and feldspar by the acidic pore fluids produces early secondary porosity within the sandstone. In addition, the acidic, cation free pore waters leach and degrade the authigenic illite crystal lattice, hence resolving the short digitate nature of the illite laths. According to the classification scheme used by Schmidt and McDonald (1979) the Basal Quartz sandstones are in the semi-mature stage of mesodiagenesis, (Figure 5.2).

Sarkisyan (1970) states that new clay minerals do not originate in the presence of oil, hence petroleum had not yet migrated into the Basal Quartz sandstones when authigenic kaolinite was forming. Consequently, since formation of secondary porosity is approximately synchronous with the neoformation of kaolinite, (both of which occur before the bulk of petroleum migration) reservoir potential will be enhanced by the formation of secondary porosity. Nevertheless, as Kaolinite develops it fills (partially or totally) much of the remaining initial porosity. thus reducing reservoir quality to a greater extent than reservoir enhancement by secondary porosity.

Petroleum geologists often consider it favourable if kaolinite is the dominant clay mineral present within a potential reservoir. This is because kaolinite is a non-expandable clay and presents less problems during well completion, (Sarkisyan, 1970). Nevertheless Shelton (1964)

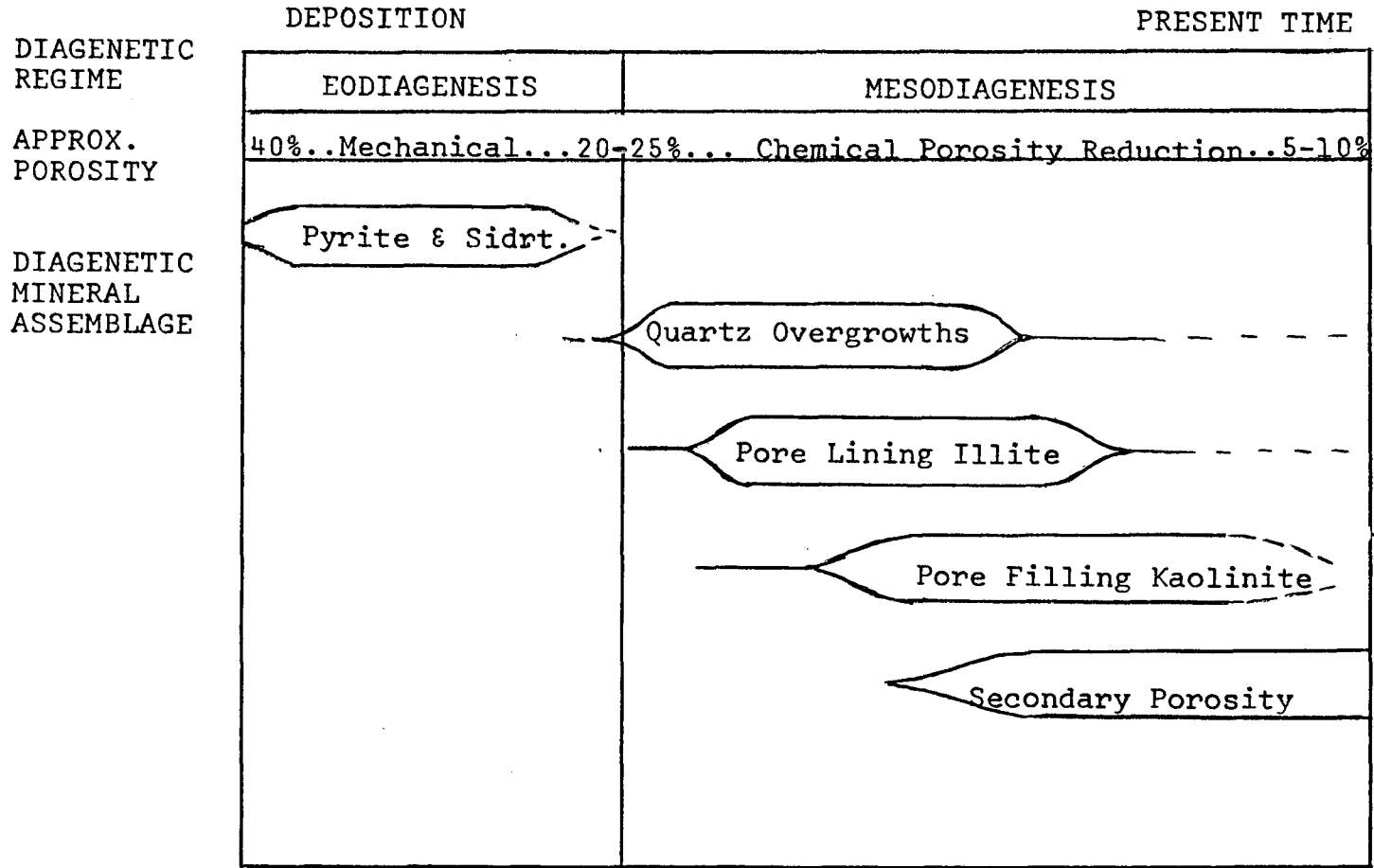
FIGURE 5.2

(After Schmidt & McDonald, 1979)



cautions against using fresh water during drilling or secondary recovery of kaolinite bearing reservoirs since permeability is reduced by dispersion of authigenic kaolinite booklets. Brines tend to have less of an effect upon authigenic kaolinite aggregates.

SUMMARY OF DIAGENESIS



CHAPTER 6CONCLUSIONS

1. The Niton Basal Quartz sediments can be divided into six different facies interpreted as having been deposited within a complex, tidally influenced, deltaic environment.
2. The quartz rich Basal Quartz sandstones, relatively free of unstable constituents, are texturally and mineralogically mature. The pre-existing sedimentary (sandstone) and metasedimentary sources of these sandstones were situated to the south and/or west of the depositional environment.
3. The bulk of the total clay fraction is of primary origin (detrital illite and kaolinite) and sand bodies deposited under conditions of high depositional energy (e.g. distributary mouth bars) have decreased detrital clay abundances, or increased initial porosity values.
4. During Mesodiagenesis the progressive assemblage of porosity and permeability reducing authigenic quartz overgrowths, pore lining illites, and pore filling kaolinites develop.

5. Authigenic illites have formed by transformation of pre-existing detrital illites and by direct precipitation out of alkaline, pore fluids, (Neoformation). Authigenic kaolinites have generally formed by neoformation in sands relatively free of detrital clay. Hence depositional energy effects favouring high initial sandstone porosity are offset by porosity reducing secondary kaolinites.
6. Acidic pore fluids, present during kaolinite neoformation, dissolve carbonate minerals thus producing secondary porosity prior to the migration of liquid hydrocarbons into the sandstones. (Secondary porosity generally occurs in sands free of detrital clay which are usually permeable to acidic pore fluids).
7. Reservoir enhancement by secondary porosity is offset by the porosity reduction effects of secondary kaolinite development.
8. It follows from conclusion three (3) that insufficient winnowing of detrital clays in low energy depositional environments concentrates clays, thus lowering initial porosity and reservoir potential. Localized areas of increased clay accumulation may also occur due to kaolinite neoformation. In conclusion, localized clay accumulation has lowered reservoir potential, but not enough to obliterate economic hydrocarbon production within the Niton Basal Quartz reservoir.

APPENDIX I

CLAY SAMPLE NUMBER	DEPTH (Feet)	KAOLINITE-ILLITE RATIO
10-14-1	6481'	42%:58%
10-14-3	6545'	79%:21%
10-14-6	6584'	52%:48%
10-14-7	6606'	56%:44%
10-14-11	6691'	72%:28%
2-18-5	6444'	99%: 1%
2-18-6	6456'	93%: 7%
2-18-9	6474'	85%:15%
2-18-10	6495'	69%:31%
2-18-11	6522'	26%:74%
2-18-13	6537'	45%:55%
4-30-2	6379'	89%:11%
4-30-4	6415'	89%:11%
4-30-5	6426'	75%:25%
4-30-6	6454'	60%:40%
4-30-8	6469'	81%:19%
4-30-9	6498'	72%:28%

BIBLIOGRAPHY

- Baylis, P., and Levinson, A.A., 1976, Mineralogical Review of the Alberta Oil Sand Deposits (Lower Cretaceous, Mannville Group): Bull. Canadian Petroleum Geol., v. 24, no. 2, p. 211-224.
- Berner, R.A., 1971, Principles of Chemical Sedimentology: New York, McGraw-Hill Book Co.
- Blatt, H., Middleton, G.V., Murray, B., 1980, Origin of Sedimentary Rocks: Englewood Cliffs, New Jersey, Prentice-Hall.
- Carrigy, M.A., and Mellon, G.B., 1964, Authigenic Clay Mineral Cements in Cretaceous and Tertiary Sandstones of Alberta: J. Sed. Petrology, v. 34, no. 3, p. 461-472.
- Collins, A.G., 1975, Geochemistry of Oilfield Waters, Developments in Petroleum Science, 1: NY, Elsevier Scientific Publishing Company.
- Füchtbauer, H., 1967, Influence of Different Types of Diagenesis on Sandstone Porosity: Reprint from The Proceedings of the Seventh World Petroleum Congress.
- Glaister, R.P., 1959, Lower Cretaceous of Southern Alberta and Adjoining Areas: Bull. Am. Assoc. Petroleum Geologists, v. 43, no. 3, p. 590-640.
- Grim, R.E., 1968, Clay Mineralogy, 2nd ed.: NY, McGraw-Hill Book Company.

- Guven, N., Hower, W.F., Davies, D., 1980, Nature of Authigenic Illites in Sandstone Reservoirs: Journal of Sedimentary Petrology, v. 50, no. 3.
- Ho and Coleman, 1969, Recent Sediments in the Atchafalaya Basin: Geological Soc. America Bull. v. 80, p. 183-192.
- Kerr, P.F., 1977, Optical Mineralogy, 4th ed.: NY, McGraw-Hill Book Company.
- Magara, K., 1978, Compaction and Fluid Migration Practical Petroleum Geology Developments in Petroleum Science, 9: NY, Elsevier Scientific Publishing Comp.
- Millot, G., 1970, Geology of Clays: NY, Springer-Verlag.
- Nelson, S.J., 1970, The Face of Time: The Geological History of Western Canada: Published by Alberta Soc. of Petrol. Geol.
- Pettijohn, Potter, Siever, 1972, Sand and Sandstone: NY, Springer-Verlag.
- Reineck, H.E., and Singh, I.B., 1973, Depositional Sedimentary Environments: NY, Springer-Verlag.
- Sarkisyan, G., 1972, Origin of Authigenic Clay Minerals and Their Significance in Petroleum Geology: Sediment. Geol., 7, p. 1-22.
- Schmidt, V., and McDonald, D.A., 1979, Secondary Reservoir Porosity in the Course of Sandstone Diagenesis: AAPG Continuing Education Course Note Series #12.
- Shelton, J.W., 1964, Authigenic Kaolinite in Sandstone: J. Sed. Petrology, v. 34, no. 1, p. 102-111.

Williams, G.D., 1963, The Mannville Group (Lower Cretaceous) of Central Alberta: Bull. Can. Petroleum Geologists, v. 11, no. 1, p. 350-368.

Wilson, M.D., and Pittman, E.D., 1977, Authigenic Clays in Sandstones: Recognition and Influence on Reservoir Properties and Paleoenvironmental Analysis: The Society of Economic Paleontologists and Mineralogists.